Cell Surface Vimentin Is an Attachment Receptor for Enterovirus 71

Ning Du,[a,c] Haolong Cong,[a] Hongchao Tian,[a,b] Hua Zhang,[a,c] Wenliang Zhang,[a,c] Lei Song,[a] Po Tien[a]

Center for Molecular Virology, CAS Key Laboratory of Pathogenic Microbiology and Immunology, Institute of Microbiology, Chinese Academy of Sciences, Beijing, People's Republic of China[a]; Anhui University, Anhui, People's Republic of China[b]; University of the Chinese Academy of Sciences, Beijing, People's Republic of China[c]

ABSTRACT

Enterovirus 71 (EV71) is a highly transmissible pathogenic agent that causes severe central nervous system diseases in infected infants and young children. Here, we reported that EV71 VP1 protein could bind to vimentin intermediate filaments expressed on the host cell surface. Soluble vimentin or an antibody against vimentin could inhibit the binding of EV71 to host cells. Accompanied with the reduction of vimentin expression on the cell surface, the binding of EV71 to cells was remarkably decreased. Further evidence showed that the N terminus of vimentin is responsible for the interaction between EV71 and vimentin. These results indicated that vimentin on the host cell surface may serve as an attachment site that mediated the initial binding and subsequently increased the infectivity of EV71.

IMPORTANCE

This study delivers important findings on the roles of vimentin filaments in relation to EV71 infection and provides information that not only improves our understanding of EV71 pathogenesis but also presents us with potentially new strategies for the treatment of diseases caused by EV71 infections.

Enterovirus 71 (EV71) is a single-stranded RNA virus that belongs to human enterovirus species A of the genus *Enterovirus* within the *Picornaviridae* family. EV71 was thought to be one of the main pathogenic agents that cause foot, hand, and mouth disease (HFMD) in young children (1–4). In recent years, outbreaks of EV71-related HFMD have been reported in Southeast or East Asia, including in Taiwan, Malaysia, Singapore, Japan, and China (5–7). Particularly, since 2008, one million EV71-related HFMD cases were reported each year in China, including hundreds of fatal cases per year. Because of its danger and high frequency of infection, EV71-related HFMD has raised considerable public health concerns (8). However, available treatments for EV71 infection are limited, as there is currently no effective chemoprophylaxis or vaccination against infection.

Unlike CA16 and other enteroviruses, EV71 infection is usually accompanied by severe neurological complications, such as aseptic meningitis, acute flaccid paralysis, encephalitis, and other rarer manifestations (2, 9, 10). The EV71-associated neurological complications can sometimes be fatal, and neurogenic pulmonary edema is thought to be the main pathogenic cause in fatal cases (11–13). It has been postulated that overwhelming virus replication in combination with tissue damage and the induction of toxic inflammatory cytokines and cellular immunity are the possible process of pathogenesis (14, 15). Although the initial viral illness often is self-limited, EV71 infection may result in long-term neurologic and psychiatric effects on the central nervous system (CNS) in children (16). EV71 infection involving the CNS, and cardiopulmonary failure may be associated with neurologic sequelae, delayed neurodevelopment, and reduced cognitive functioning (10, 16, 17).

As a nonenveloped virus, EV71 enters host cells via a receptor-mediated clathrin-dependent endocytotic pathway (18). Several kinds of cell receptors for EV71 have been identified. Human P-selectin glycoprotein ligand-1 (PSGL-1) and scavenger receptor B2 (SCARB2) are two functional receptors believed to determine EV71 host range and tissue tropism (19, 20). PSGL-1 is a sialomucin membrane protein expressed on leukocytes which have a major role in the early stages of inflammation (21–23). The tyrosine sulfation at the N-terminal region of PSGL-1 has been proven to interact with EV71 and thus may facilitate virus entry (24). Human SCARB2, the second reported cell receptor for EV71, belongs to the CD36 family (25, 26). SCARB2 is one of the most abundant proteins in the lysosomal membrane and participates in membrane transport and the reorganization of the endosomal and lysosomal compartments (27). PSGL-1 is expressed mainly on neutrophils, monocytes, and most lymphocytes, while SCARB2 is widely expressed on most types of cells, including neurons (19, 20). Amino acids (aa) 144 to 151 of SCARB2 have been proven to be critical for binding to EV71 VP1 (28). Thus, SCARB2 is believed to be directly involved in EV71 infection of the brain. In addition, SCARB2 can be utilized by most EV71 strains as an entry receptor, while PSGL-1 can mediate infection only by certain strains. More EV71 virus binds to mouse L cells that express human PSGL-1 (L-PSGL-1 cells) than to mouse L cells that express human SCARB2 (L-SCARB2 cells) due to a higher affinity of PSGL-1 for the virus. However, EV71 could infect L-SCARB2 cells more efficiently than L-PSGL-1 cells (29, 30). SCARB2 is capable of virus binding, virus internalization, and virus uncoating, while PSGL-1 is capable only of virus binding (30). Thus, PSGL-1 may act as a binding receptor but not an uncoating receptor for EV71. Other receptors, such as sialylated glycan and annexin II, have also been shown to facilitate EV71 infection in various kinds of cells,

and cell surface heparan sulfate glycosaminoglycan was recently reported to be an attachment receptor for EV71 in RD cells (31, 32); however, as inhibition of these receptors by antagonists did not completely abolish EV71 infection, it was suggested that multiple receptors are involved during EV71 infection. Vimentin is the major intermediate filament protein of astrocyte cells and cells adapted to tissue culture (33). An increasing number of reports recognized an important role for cell surface vimentin as a component of the pathogen attachment and endocytotic pathways (34–39). In this study, we further demonstrate that EV71 VP1 specifically binds to the vimentin intermediate filament located on the cell surface and that the vimentin expressed on the cell surface is involved in the attachment of EV71 to host cells.

MATERIALS AND METHODS

Reagents and antibodies. N-Decyl-β-D-maltopyranoside (DDM) was obtained from Affymetrix, California. Protease inhibitor cocktail and anti-SCARB2 antibody were obtained from Sigma-Aldrich, Missouri. Anti-EV71 monoclonal antibody was obtained from Millipore, Massachusetts. Anti-PSGL-1 antibody was obtained from R&D Systems, Minnesota. FuGENE transfection reagent was obtained from Roche, Indiana. Rabbit antivimentin polyclonal antibody, mouse antivimentin, mouse anti-β actin, mouse anti-glutathione S-transferase (GST), mouse anti-Flag monoclonal antibody, rhodamine (tetramethyl rhodamine isocyanate [TRITC])-conjugated anti-rabbit IgG antibody, fluorescein isothiocyanate (FITC)-conjugated anti-rabbit IgG antibody, FITC-conjugated anti-mouse IgG, horseradish peroxidase (HRP)-conjugated anti-mouse IgG, and HRP-conjugated anti-rabbit IgG used in immunofluorescence studies, infection inhibition assays, and Western blot analyses were all obtained from Santa Cruz Biotechnology, California. PSGL-1 and SCARB2 protein used in infection inhibition assays were obtained from Sino Biological, Beijing, China.

Cell culture, virus isolates, and virus infection. The prototype enterovirus 71 (EV71) BrCr strain was a gift from Qi Jin (Institute of Pathogen Biology, Chinese Academy of Medical Sciences, Beijing, People's Republic of China). The prototype EV71 clinical strains Hunan 09 and HeN 09 were gifts from Zhang Bo (Wuhan Institute of Virology, Chinese Academy Of Sciences, Wuhan, People's Republic of China). The human astrocytoma (U251) cell lines, human rhabdomyosarcoma (RD) cells, African green monkey kidney epithelial (Vero) cells, human cervical (HeLa) cells, human T lymphocyte (Jurkat) cells, and mouse embryonic fibroblast (3T3) cells were propagated and maintained in either double modified Eagle's medium (DMEM), modified Eagle's medium (MEM), or 1640 medium, all supplemented with antibiotics (penicillin and streptomycin) and 10% fetal bovine serum (Invitrogen, California), at 37°C in the presence of 5% CO_2. In all experiments, cells (other than 3T3 cells) were infected with the respective virus at a multiplicity of infection (MOI) of 4 PFU cell^{-1}. The 3T3 cells were infected at an MOI of 20.

Plasmids and protein expression. To create the expression vectors expressing either EV71 VP1, VP2, VP3, or 3C, EV71 genomic RNA was extracted from the culture fluid of virus-infected RD cells using a virus genome extraction kit. Single-stranded cDNA was then synthesized from the purified virus RNA by reverse transcription (RT) (Promega). Each of the VP1, VP2, VP3, and 3C genes was amplified from the cDNA by PCR over 34 cycles of denaturation at 98°C for 10 s, primer annealing at 55°C for 30 s, and extension at 72°C for 1.5 min, using VP1 sense primer 5′-CGCGGATCCGACAGAGT GGCAGATGTGATTG-3′ and antisense primer 5′-CCGGAATTCTTAGAG CGTAGTGATTGCCGTTC-3′, VP2 sense primer 5′-CCCAAGCTTTCTCC CTCTGCTGAAGCATGTGGC-3′ and antisense primer 5′-CCCAAGCTTT TACTGCGTAACTGCCTGCCTGAGAC-3′, VP3 sense primer 5′-CCCAA GCTTGGTTTCCCCACTGAATTGAA-3′ and antisense primer 5′-ACGCG TCGACTTATTGAATAGTGGCCGTTTGC-3′, and 3C sense primer 5′-CG CGGATCCCCCAGCTTAGACTTCGCCTTGTCT-3′ and antisense primer 5′-CCGGAATTCTTATTGCTCGCTGGCAAAATAACTCCT-3′. Each of

the PCR products was separated by electrophoresis in 1.0% agarose gels, gel purified, and then cloned into the corresponding restriction sites of the pcDNA-Flag vector to produce plasmids expressing VP1-Flag, VP2-Flag, VP3-Flag, and VP3C-Flag.

To create expression vectors expressing either vimentin or 3C, the full-length VP1 and 3C cDNAs were generated by PCR using the VP1 sense primer 5′-CGGAATTCTCCACCAGGTCCGTGTCCTCG-3′ and antisense primer 5′-CGGCGGCCGCTCTTCAAGGTCATCGTGATGT G-3′ and 3C sense primer 5′-CGGAATTCCCCAGCTTAGACTTCGCC TTGTCT-3′ and antisense primer 5′-GCGGCCGCTTTGCTCGCTGGC AAAATAACTCCT-3′. The PCR products were separately cloned into the pGEX-4T-1 expression vector. Full-length human and mouse vimentin cDNA and the truncated human vimentin cDNA sequences were generated by PCR using these primers: vimentin (1 to 230) sense primer 5′-C GGGATCCGTCACCAGGTCCGTGTCCTCG-3′ and antisense primer 5′-CCCAAGCTTCTCTTCTTGCAAAGATTCCAC-3′, vimentin (231 to 467) sense primer 5′-CCCAAGCTTTTCAAGGTCATCGTGATGCT G-3′ and antisense primer 5′-CCCAAGCTTGGCGAAGCGGTCATTCA GCTC-3′, vimentin (116 to 230) sense primer 5′-CGGGATCCGAA CTACATCGACAAGGTGCGC-3′ and antisense primer 5′-CCCAAGC TTCGAGGCGTAGAGGCTGCGGCT-3′, and vimentin (1 to 56) sense primer 5′-CGGGATCCG TCCACCAGGTCCGTGTCCTCG-3′ and ant isense primer 5′-CGGGATCCGTCCCCGGGCGGCGTGTATGCC-3′. The respective PCR products were cloned into the pET20b vector and expressed in *Escherichia coli* BL21. Solubilizing and refolding of the recombinant proteins in the inclusion body was performed as described before (40–42). The recombinant proteins were purified using affinity chromatography (Ni-nitrilotriacetic acid [NTA] or glutathione-Sepharose [GE]) followed by size exclusion chromatography (Superdex 200; GE Healthcare).

Cell vimentin knockdown experiment. In order to elucidate potential roles for vimentin in EV71 infection, a vimentin knockdown cell line (VK-U251) was constructed using a retrovirus vector that stably expressed the small interfering RNA (siRNA) specific to vimentin. To build VK-U251, a short hairpin RNA (shRNA) targeting the human vimentin (shVim) gene as reported previously and a control shRNA (shControl) were designed (43). In order to facilitate the formation and processing of the shRNA, a loop sequence (TTCAAAGAGA) was designed in the middle area of all shRNAs. The sequences of the two shRNAs were as follows: shVim, 5′-GATCCGCTATGTGACCACATCCACTTCAAGAGAGTGG ATGTGGTCACATAGCTTTTTTG-3′; and shControl, 5′-GATCCCC ACCATGCACGTATGTCATTCAAGAGATGACATACGTGCATGGT GGTTTTTTG-3′. The corresponding complementary oligonucleotides were also synthesized to produce DNA duplexes of each of the shRNAs. The shRNA oligonucleotides were annealed and ligated to the BamHI and EcoRI sites behind the human U6 promoter of pSIREN-RetroQ vector, and the constructs were confirmed by DNA sequencing. Phoenix cells were plated and transfected with the resultant pSIREN-RetroQ-siVim or pSIREN-RetroQ-siControl plasmid in the presence of a helper plasmid by using the FuGENE transfection reagent. At 48 h posttransfection, cell culture fluid containing the recombinant retroviruses were harvested and used to infect U251 cells. The infected cells were screened using puromycin at a concentration of 5 µg ml^{-1}. Vimentin expression in VK-U251 and control cells (C-U251) was analyzed by Western blot analysis. To decrease vimentin expression in mouse 3T3 cells, the cells were transfected with the siRNA control or siRNA specific to mouse vimentin (44). The expression levels of vimentin were determined by Western blot analysis.

Virus propagation, purification, and titer determination. Virus was propagated and purified as described before (45). To determine virus titers, RD cells were plated into 96-well dishes, incubated overnight, and then infected with the serially diluted virus. After adsorption for 30 min, the virus suspension was replaced with modified Eagle's medium containing 2% fetal bovine serum. The cultures were incubated at 37°C for 5 days, and plates that displayed cytopathic effects were counted. Virus titers were determined by the Reed-Muench method. All virus titer data presented

are means ± standard deviations (SD) based on three independent experiments.

Western blotting, pulldown assay, and coimmunoprecipitation. Western blotting and pulldown assays were performed as described before (46). For coimmunoprecipitation, cell lysates were prepared and preimmunoprecipitated with protein G-agarose beads. After a short centrifugation, the precipitates were either incubated with mouse IgG-conjugated agarose beads, EV71-conjugated agarose beads, or vimentin monoclonal antibody-conjugated agarose beads. After 2 h of incubation at 4°C, the beads were washed with lysis buffer and heat denatured in sample-loading buffer (50 mM Tris-HCl [pH 6.8], 100 mM dithiothreitol [DTT], 2% SDS, 0.1% bromophenol blue, and 10% glycerol). After a brief centrifugation, the proteins in supernatants were separated by SDS-PAGE followed by Western blot analysis. The blots were developed using the chemiluminescence reaction (GE Healthcare).

Quantitative RT-PCR, indirect immunofluorescence, and flow cytometry. Quantitative RT-PCR and indirect immunofluorescence analysis were performed as described before (47, 48). For flow cytometry, cells were harvested at the indicated times and fixed in 0.01% formaldehyde for 10 to 15 min at room temperature. After three washes in phosphate-buffered saline (PBS), the cells were permeabilized with 0.1% NP-40 in PBS for 20 min. Cells were blocked with 5% bovine serum albumin (BSA) in PBS and incubated for 1 h at room temperature. After being washed, the cells were resuspended in PBS with 1% BSA and incubated for 2 h at 4°C with the primary antibody at a final concentration of about 1 μg ml^{-1}. Cells were then incubated for 1 h with the fluorescent secondary antibody. The cells were then subjected to flow cytometry analysis after they had been washed with PBS. For cell surface staining, the cells were not permeabilized, but the other steps remained the same.

Virus binding inhibition assay. To examine the effect of soluble vimentin on virus binding to host cells during infection, we mixed EV71 with either vimentin or BSA and incubated them for 60 min at 4°C prior to infection. The cells were then incubated with the above-described treated EV71 at 4°C for 1 h, washed three times with culture medium, and subjected to flow cytometry or Western blot analysis.

To examine the inhibition effects of pretreating host cells with specific antibodies on virus binding, the cells were preincubated with polyclonal antibody against either vimentin, SCARB2, PSGL-1, or rabbit IgG for 60 min at 4°C before being incubated with EV71 for 1 h at 4°C. The cells were then subjected to flow cytometry or Western blot analysis as mentioned above.

To study the effects of vimentin and vimentin antibody on virus replication, cells were incubated with EV71 at 4°C for 1 h in the presence of either vimentin or vimentin antibody. Then, fresh medium was added to the infected cells, and infection was allowed to proceed for the indicated times at 37°C. Virus replication of the infected cells was determined by measuring the virus titers in the culture fluids and cell lysates.

Statistical analysis. Data were subjected to one-way analysis of variance with factors of treatment and expressed as means ± SD. Comparisons between any two groups were performed by unpaired Student's t tests: **, significant difference at P values of <0.02 compared with the control; *, significant difference at P values of <0.05 compared with the control.

RESULTS

To investigate whether EV71 can interact directly with vimentin, we incubated U251 cell lysates with EV71 strain BrCr particles immobilized on agarose beads conjugated with anti-EV71 VP1 monoclonal antibody and analyzed the precipitated proteins by Western blotting. The results (Fig. 1A) showed that a 55-kDa band corresponding to vimentin was detected by a vimentin monoclonal antibody, whereas no vimentin was detected in the IgG and control groups. This interaction between EV71 and vimentin was further verified by a coimmunoprecipitation experiment which showed that EV71 coimmunoprecipitated with vimentin (Fig. 1B).
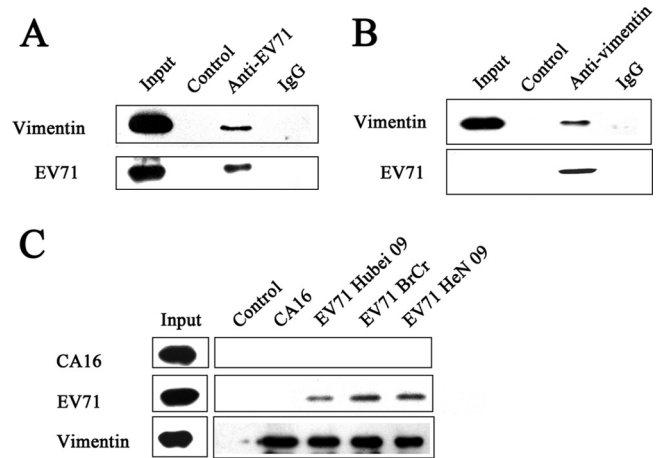

FIG 1 Experiments showing specific interaction between EV71 and cellular vimentin. (A) Detection of specific interactions between EV71 BrCr virus particles and cellular vimentin in uninfected U251 cell lysates by immunoprecipitation assays and Western blotting performed as described in Materials and Methods. The figure shows a Western blot of the following precipitated protein samples using anti-EV71 VP1 and antivimentin antibodies: input, untreated cell lysate; control, cell lysate incubated with agarose beads treated with purified EV71 particles; anti-EV71, cell lysate incubated with anti-EV71 VP1 monoclonal antibody-conjugated agarose beads treated with purified EV71 particles; IgG, cell lysate incubated with mouse IgG-conjugated agarose beads treated with purified EV71 particles. (B) Detection of specific binding of EV71 with vimentin in EV71-infected U251 cells using coimmunoprecipitation assays. U251 cells were infected with EV71 and lysates prepared as described in Materials and Methods. Infected cell lysates were then incubated with either mouse IgG or vimentin monoclonal antibody (antivimentin)-conjugated agarose beads for 2 h at 4°C. The precipitated proteins were blotted with anti-EV71 VP1 and antivimentin antibodies. Input, EV71 and vimentin markers; control, proteins from cell lysate incubated with IgG-conjugated agarose beads; antivimentin, proteins from cell lysate incubated with vimentin monoclonal antibody-conjugated agarose beads. (C) Analysis of the specific interactions between various strains of EV71 viruses and U251 cellular vimentin by immunoprecipitation assays. CA16, EV71 BrCr, EV71 Hubei 09, and EV71 HeN 09, cell lysates incubated with antivimentin monoclonal antibody-conjugated agarose beads treated with purified CA16, EV71 BrCr, EV71 Hubei 09, and EV71 HeN 09 particles, respectively; control, cell lysate incubated with agarose beads treated with purified EV71 BrCr particles.

Neither EV71 nor vimentin was detected in the IgG control group. These results thus indicated that EV71 can interact directly with vimentin. To determine whether the interaction with vimentin was specific to the test virus strain or is a feature common to other circulating EV71 strains in general, we tested two other EV71 clinical isolates for their interaction with vimentin by coimmunoprecipitation as described above. The results showed that both of these strains, which belong to the C4 genotype of EV71, were captured by vimentin and migrated at the appropriate size position in a Western blot probed with the anti-EV71 antibody (Fig. 1C). This interaction with vimentin was shown to be specific for EV71, as a parallel coimmunoprecipitation experiment with coxsackievirus A16 (CA16), another common pathogen of HFMD belonging to the same species of human enterovirus A, failed to capture the CA16 virus (Fig. 1C).

To determine if vimentin could act as an attachment receptor for EV71 entry, we first investigated the cell surface expression of vimentin by flow cytometry and immunofluorescence studies. The cytometry results (Fig. 2A) showed that there were strong immunofluorescence signals in the EV71 permissive U251, Vero,
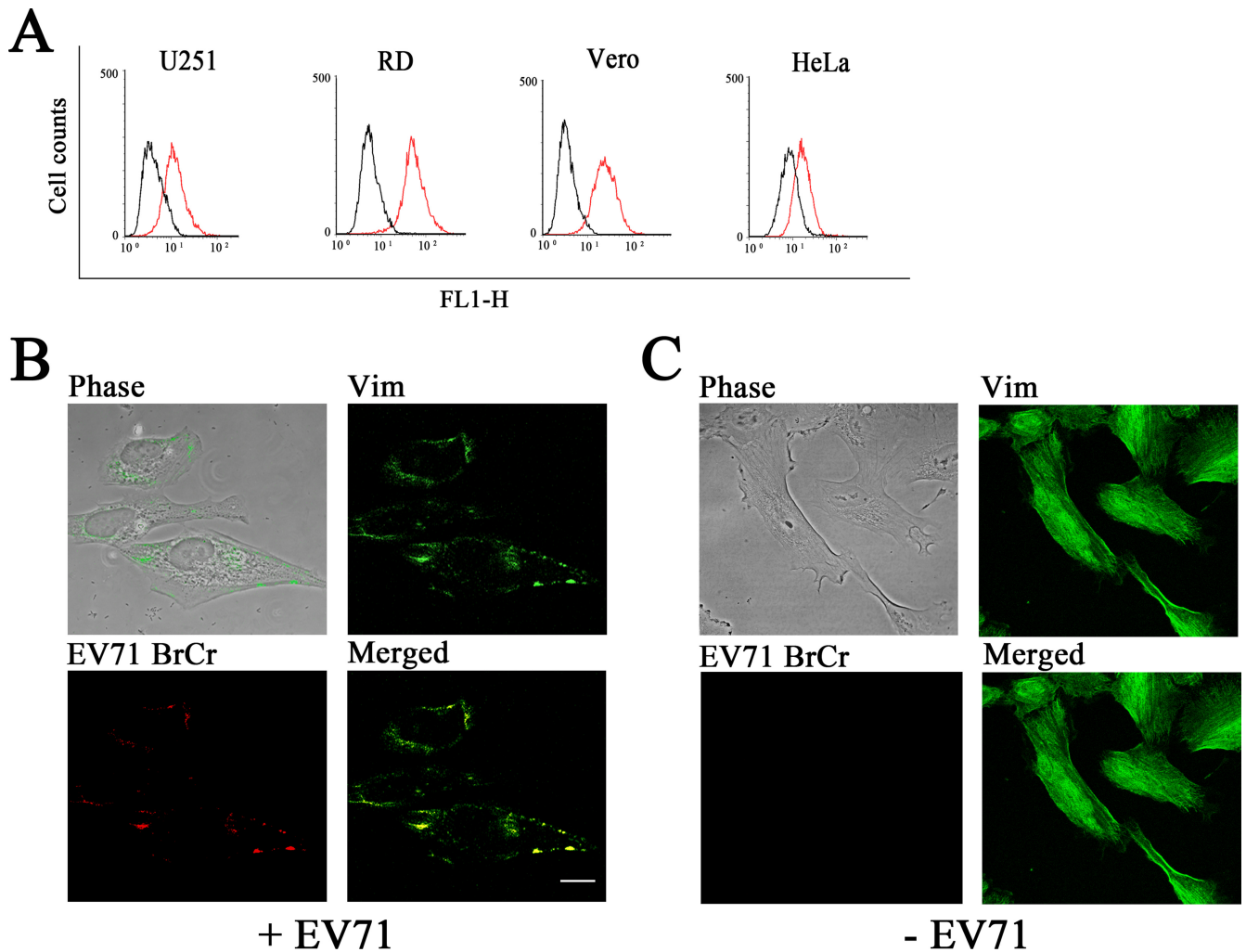
FIG 2 (A) Detection of vimentin expression on the cell surface of U251, RD, Vero, and HeLa cells by flow cytometry. Cells were fixed and incubated with either mouse IgG (black line) or antibody to vimentin (red line). The cells were then incubated with the fluorescent secondary antibody and subjected to flow cytometry analysis as described in Materials and Methods. y axis (counts) = cell counts; x axis (FL1-H) = fluorescence density. (B) Analysis of the cell surface distribution of vimentin and cell surface-bound EV71 by indirect immunofluorescence in U251 cells. Cells were infected with EV71 BrCr (+EV71) at 4°C for 1 h and then stained with specific antibody to either EV71 (red) or vimentin (green) and analyzed by confocal fluorescence microscopy. Bar = 20 μm. (C) Analysis of the distribution of cell vimentin by indirect immunofluorescence in U251 cells (−EV71). Cells were fixed and permeabilized as described in Materials and Methods. Cells were then stained with antibodies to vimentin (Vim; green fluorescence) and EV71 (red florescence) and subjected to confocal microscopy analysis. An overlay of the vimentin and EV71 florescence is also shown (merged). Cell morphology (phase) was assessed by light microscopy.

RD, and HeLa cells when stained with the vimentin antibody but not in the corresponding cells stained with mouse IgG, indicating that vimentin was expressed on the surface of these cells. However, the amounts of cell surface vimentin in RD and Vero cells were greater than those in U251 and HeLa cells. Additionally, immunofluorescence studies of nonpermeabilized U251 cells stained with vimentin monoclonal antibody demonstrated that some vimentin was located on the surface of these cells (Fig. 2B). The results showed that when EV71 was incubated with nonpermeabilized cells, the rhodamine-labeled EV71 was found localized on the cell surface and was colocalized with the cell surface vimentin stained with FITC (Fig. 2B). In contrast, when U251 cells were stained with vimentin antibody in the permeabilized states, the vimentin filaments were seen to be distributed throughout the cytoplasm (Fig. 2C).

We next determined whether EV71 binds to vimentin through its VP1 protein, the most external, surface accessible, and immunodominant protein that is believed to be responsible for host-virus binding. A pulldown assay was initially performed to analyze the interaction between VP1 and vimentin. As shown in Fig. 3A, a band representing vimentin could be detected in the eluate of cell lysates from the VP1 binding column. In contrast, no such protein band was observed in eluate from the control resins. To determine whether EV71 VP1 could directly bind with vimentin, pulldown assays were performed by incubating VP1 with vimentin protein immobilized on antivimentin monoclonal antibody-conjugated agarose beads. The results showed the presence of a VP1-GST protein band in the eluate from vimentin binding resins but not in control GST eluate (Fig. 3B). The capsid of EV71 consists of 60 subunits comprising the four capsid proteins VP1, VP2, VP3, and VP4. VP1, VP2, and VP3 are exposed on the virion surface and believed to mediate cell receptor binding or endocytosis (49). To
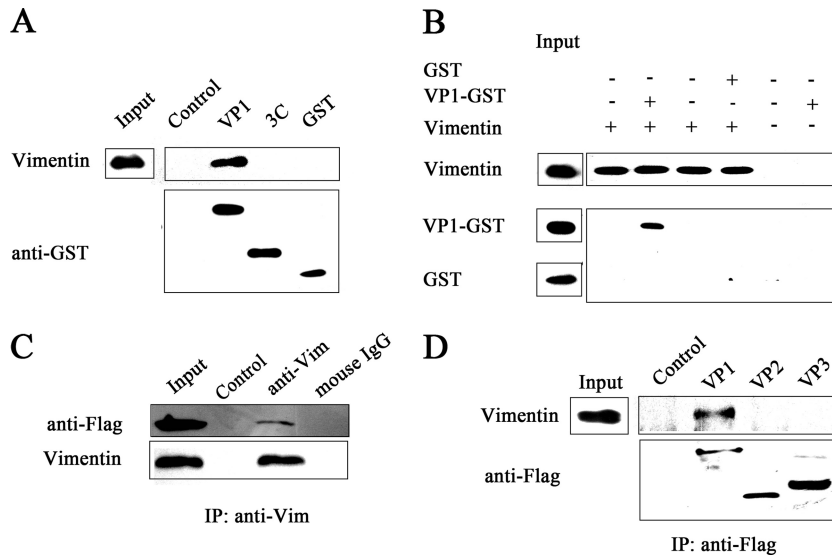
FIG 3 Experiments showing the interaction between EV71 VP1 protein and vimentin. (A) Detection of binding between VP1 and vimentin using GST pulldown assays and Western blotting. The eluates obtained as described in Materials and Methods were blotted with antivimentin and anti-GST antibodies, and the resultant VP1 protein band observed is indicated. Input, untreated cell lysate; control, U251 cell lysate incubated with glutathione-Sepharose beads; VP1, 3C, and GST, U251 cell lysate incubated with VP1-GST, 3C-GST, or GST precombined glutathione-Sepharose beads, respectively. (B) Pulldown assays and Western blot analysis showing the interaction between VP1 and vimentin. GST or VP1-GST protein was incubated with antivimentin monoclonal antibody-conjugated agarose beads that were preincubated with vimentin protein. The precipitated proteins were blotted with antibodies to either vimentin or GST, and the resultant VP1-GST protein band observed is indicated. (C) Analysis of the binding of VP1 to vimentin by coimmunoprecipitation and Western blotting. U251 cells were transfected with a plasmid expressing VP1, lysed, and coimmunoprecipitated with vimentin antibodies (anti-Vim) or mouse IgG. The precipitated proteins were blotted with antibodies to vimentin and EV71 VP1. Input, cell lysate; control, agarose beads incubated either with no antibodies or with IgG; anti-Vim and mouse IgG, agarose beads incubated with vimentin antibody and mouse IgG, respectively. (D) Coimmunoprecipitation and Western blot analysis of the binding of vimentin to VP1, VP2, and VP3. U251 cells were transfected with plasmids expressing either VP1, VP2, or VP3. Coimmunoprecipitation was performed with Flag antibody. The precipitated proteins were analyzed by Western blotting using antibodies to vimentin and Flag. Control, precipitated proteins from cells with no plasmid transfection; VP1, VP2, VP3, precipitated proteins from cells transfected with VP1, VP2, VP3 plasmids, respectively. The figure shows only EV71 VP1 interacted with vimentin and not VP2 or VP3.

investigate which capsid protein mediates the interaction between the EV71 particles and vimentin, we transfected U251 cells with plasmids expressing either VP1-Flag, VP2-Flag, or VP3-Flag. Co-immunoprecipitation experiments performed on these cells followed by Western blot analysis using antivimentin and anti-Flag antibodies showed that vimentin could be precipitated by VP1-Flag but not VP2-Flag or VP3-Flag (Fig. 3C and D). Together, these studies provided strong evidence that EV71 VP1 could bind directly and specifically to vimentin and that the EV71 VP1 mediated the interactions between the EV71 particle and cell surface vimentin.

An assay was done to investigate if the addition of exogenous vimentin would competitively inhibit the binding of the virus to host cells and thus virus infection, EV71 was preincubated with either vimentin (0, 5, 10, 20, 30, and 40 μg ml^{-1}) or BSA (40 μg ml^{-1}) for 60 min at 4°C before being used to infect U251 cells (MOI of 4). At 1 h postinfection, samples of the cells were washed three times with culture medium and analyzed for bound virus particles by Western blotting and flow cytometry. The blotting results (Fig. 4A) showed that preincubation with exogenous vimentin reduced the binding of EV71 particles to the cells compared to preincubation with BSA. This inhibition effect was specific to EV71, as exogenous vimentin failed to block the binding of CA16 to U251 permissive cells (Fig. 4A). Analysis by flow cytometry showed that preincubation with vimentin at a concentration of 10 μg ml^{-1} dramatically reduced the amount of EV71 binding on the U251 cell surface, while preincubation with BSA had no

effect (Fig. 4B). The binding of EV71 to U251 cells was also analyzed by using quantitative PCR, and the results showed that the EV71 RNA levels observed were inversely proportional to the concentrations of soluble vimentin added. However, the reduction of EV71 RNA levels was not observed when the concentration of vimentin was increased from 10 μg ml^{-1} to 20 μg ml^{-1} (Fig. 4C). Similarly, the virus yields in both the culture medium and infected cells were significantly reduced, and the levels of reduction were proportional to the concentrations of vimentin added (Fig. 4D). Moreover, the lower virus yields in the vimentin-pretreated cells were associated with an attenuation of the typically severe cytopathic effect (CPE) of EV71 seen in the infected untreated control or the BSA-pretreated cells. These results indicated that preincubation with exogenous vimentin competitively inhibited EV71 infection (Fig. 4E). To further understand the effect of exogenous vimentin on EV71 infection, the binding of EV71 was measured by quantitative PCR in U251 cells treated with vimentin at a concentration of 20 μg ml^{-1} at various times after the initiation of infection. The results showed that the binding of EV71 to the cells decreased proportionately with the increased time delay in treatment with vimentin postinfection, such that treatment at 30 min postinfection had no significant effect on EV71 binding (Fig. 4F). These results indicated that the inhibitory effect of exogenous vimentin was at the binding stage of EV71 to U251 cells.

The question of whether vimentin also participates in the binding of EV71 in the infection of HeLa, Vero, and RD cells, the most well-known permissive cell lines for EV71 infection and replica-
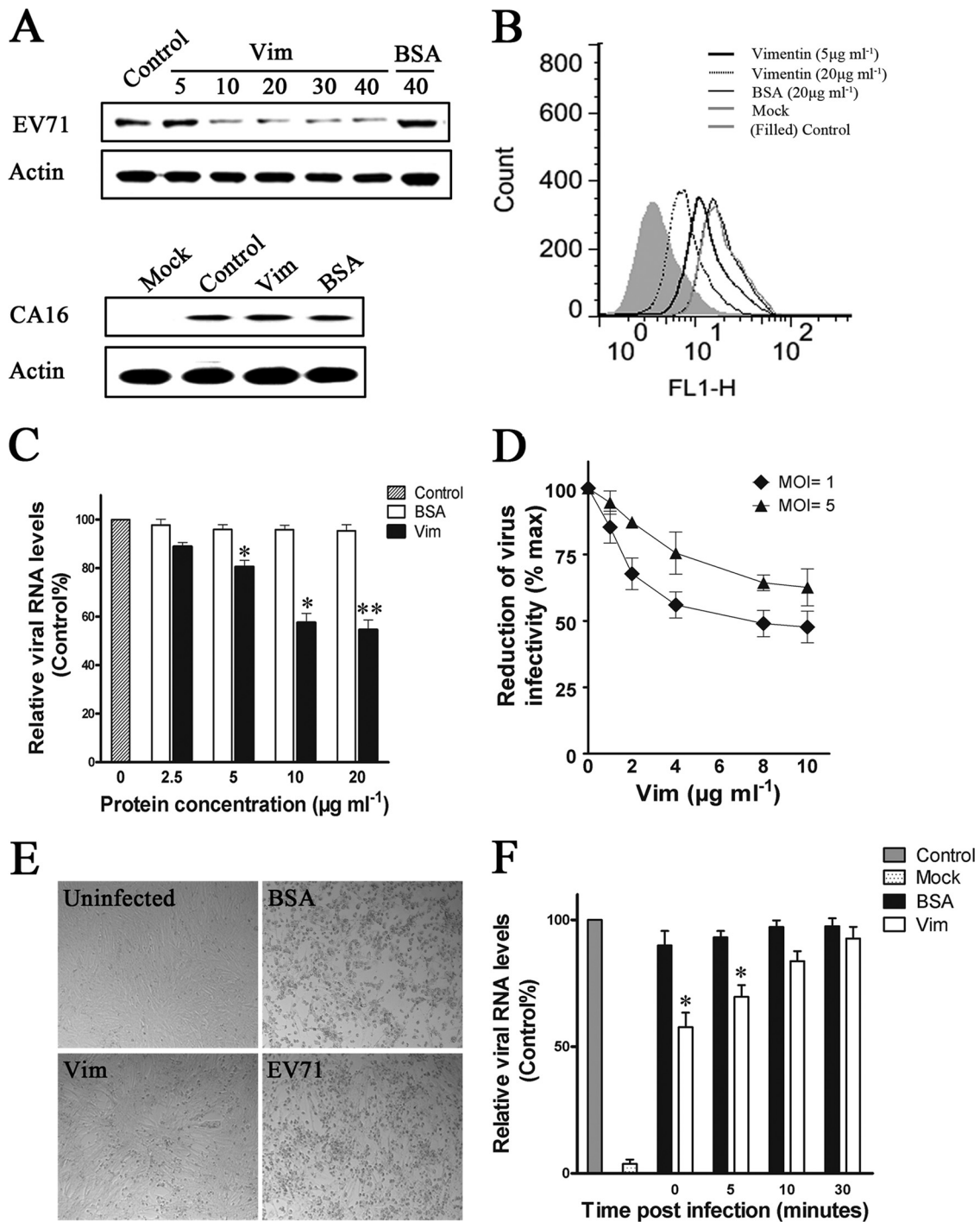
FIG 4 Experiments on the role of vimentin in the attachment of EV71 to U251 cells. (A) Analysis of the binding of EV71 or CA16 to U251 cells using competitive inhibition assays and Western blotting. Cells were infected with EV71 or CA16 at 4°C for 1 h after the virus inoculum was preincubated with vimentin or BSA at the concentrations indicated (µg ml^{-1}). Control, cells infected with untreated virus. Infected cell lysates were subjected to Western blot analysis using antibodies to EV71, CA16, and β-actin (internal control). The figure shows the inhibition of EV71 binding but not CA16 binding after pretreatment of the virus inoculum with vimentin. (B) Flow cytometry analysis of the binding of EV71 to U251 cells after pretreatment of the virus inoculum with increasing concentrations of vimentin (5 µg ml^{-1}, black heavy line; 20 µg ml^{-1}, black dotted line) or BSA (20 µg ml^{-1}, gray hairline). Black hairline (mock), infected cells with no vimentin or BSA added. Gray filled line (control), cells with no EV71 infection. x axis (FL1-H) = fluorescence density. (C) Analysis of the binding of EV71 to U251 cells using quantitative RT-PCR. Cells were infected with EV71 at 4°C for 1 h after the virus inoculum was preincubated with vimentin or BSA at the concentrations indicated. Control, cells infected with untreated EV71. (D) Infectivity of vimentin-pretreated EV71 in U251 cells. EV71 was pretreated with various doses of vimentin (Vim) at 4°C for 1 h prior to infecting U251 cells. The total virus yield at 48 h postinfection was determined. Virus titer from cells infected with EV71 that had no vimentin pretreatment was used as a reference (100%) to calculate the percent reduction in 50% tissue culture infective dose (TCID$_{50}$) in the vimentin-pretreated groups. (E) CPE of EV71 infections viewed under the visible light phase microscope, showing representative fields of control uninfected U251 cells (uninfected), cells infected with either untreated EV71 (EV71), vimentin-pretreated EV71 (Vim; 20 µg ml^{-1}) or control BSA-pretreated cells (BSA; 20 µg ml^{-1}). (F) Analysis of the influence of vimentin on the binding of EV71 to U251 cells using quantitative RT-PCR. Cells were infected with EV71 at 4°C. Vimentin (20 µg ml^{-1}) or BSA (20 µg ml^{-1}) was then added to the cell culture at the indicated time postinfection. All cells were harvested at 60 min postinfection, and the binding of EV71 was then analyzed using quantitative RT-PCR.
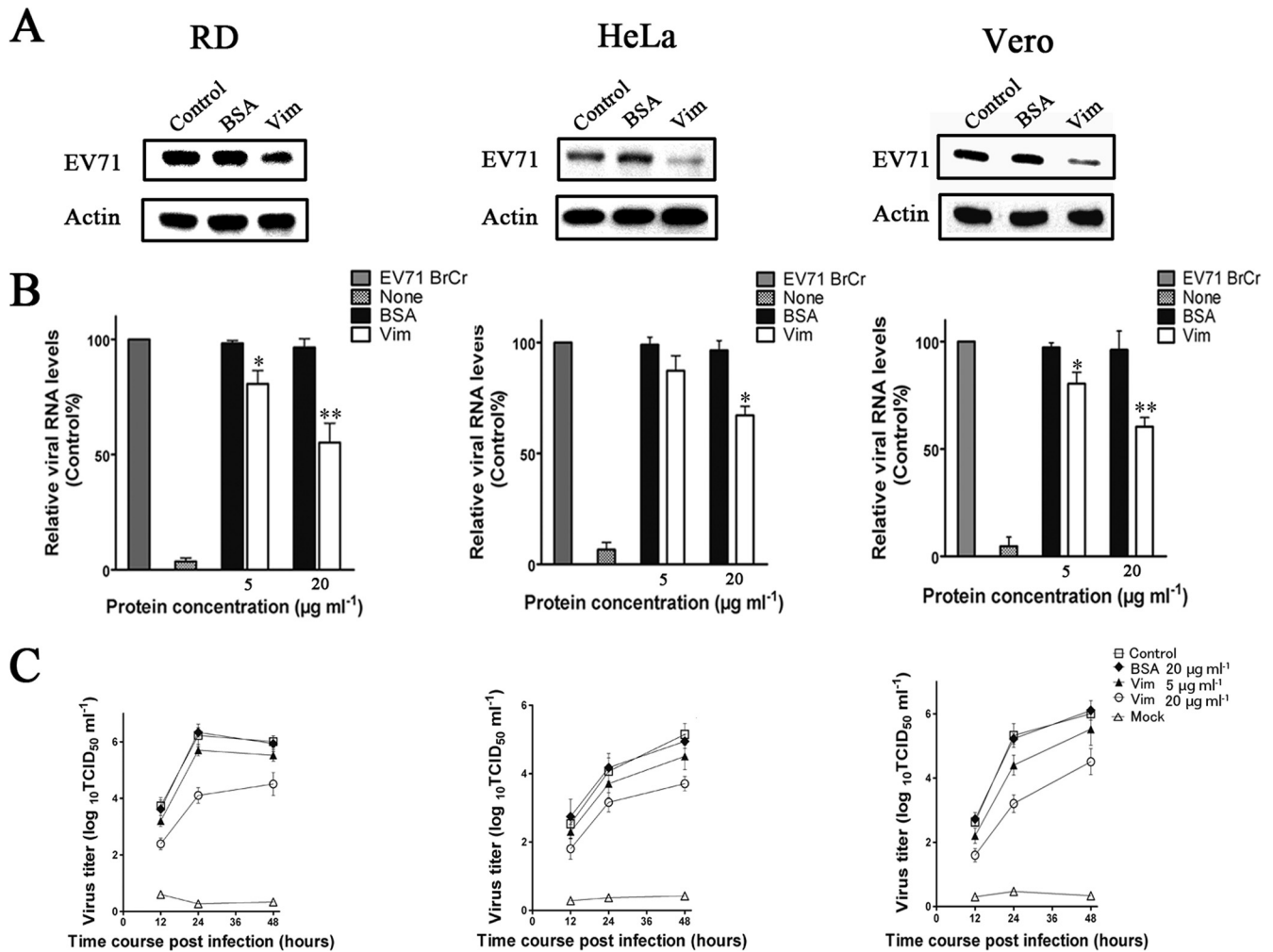
FIG 5 Analysis of the role of vimentin in the attachment of EV71 to RD, HeLa, and Vero cells. (A) Western blot analysis of the inhibition of EV71 infection after pretreating the virus inoculum with vimentin (Vim) or BSA. Cells were infected with EV71 at 4°C for 1 h, lysed, and Western blotted with antibody to EV71 and β-actin (internal control) as described in Materials and Methods. Control, cells infected with untreated virus; BSA, cells infected with BSA-pretreated virus; Vim, cells infected with vimentin-pretreated virus. (B) Analysis of the binding of EV71 to cells using quantitative RT-PCR. Control, cells infected with untreated virus; mock, cells incubated with no virus. (C) Infectivity of vimentin-pretreated EV71 in RD, HeLa, and Vero cells. EV71 was pretreated with vimentin or BSA at 4°C for 1 h prior to infecting the cells. The total virus yield at 12, 24, and 48 h postinfection at 37°C was determined. Control, cells infected with untreated virus; BSA, cells infected with BSA-treated virus; Vim, cells infected with vimentin-treated virus; mock, cells incubated with no virus.

tion, was investigated. Virus columns were preincubated with either vimentin (20 µg ml^{-1}) or BSA (20 µg ml^{-1}) for 60 min at 4°C before being used to infect U251 cells, and the amounts of virus particles bound to the cells were determined at 1 h postinfection by Western blotting and quantitative PCR. The results showed that preincubation with vimentin also inhibited the binding of EV71 to HeLa, Vero, and RD cells as reflected in the reduction of both the EV71 protein fluorescence signals and EV71 RNA levels in infected cells pretreated with vimentin compared to those pretreated with BSA (Fig. 5A and B). Moreover, the inhibition effect of vimentin observed in these cell types was collaborated by a reduction in virus yield when they were infected with vimentin-pretreated EV71 (Fig. 5C). However, the levels of reduction in EV71 binding and virus yields differed between the cell types. The decrease in EV71 binding and virus yield was greater in RD and Vero cells than in HeLa cells (Fig. 5B and C).

To provide further evidence for the participation of cell surface vimentin in EV71 infection, U251 cells were preincubated with either a polyclonal antibody to vimentin (0, 20, 40, 60, and 80 µg ml^{-1}) or the isotype IgG (80 µg ml^{-1}) for 45 min before being infected with EV71. After infecting for 1 h at 4°C, samples of the cells were subjected to Western blot analysis. The blotting results (Fig. 6A) indicated a partial inhibition of EV71 binding as reflected by a decrease in VP1 proteins observed in cells preincubated with vimentin antibody, while no change was detected in the corresponding rabbit IgG preincubated cells. In addition, the lower virus yield obtained in the vimentin antibody-pretreated cells was associated with an attenuation of the typical CPE observed in the EV71-infected untreated control or the isotype antibody-pretreated cells (Fig. 6B). The binding of EV71 to U251 cells was also measured by quantitative PCR, and the results indicated a partial inhibition of EV71 binding as reflected in a decrease in EV71 RNA levels (Fig. 6C). However, preincubating cells with vimentin antibody at a concentration of 60 µg ml^{-1} did not de-
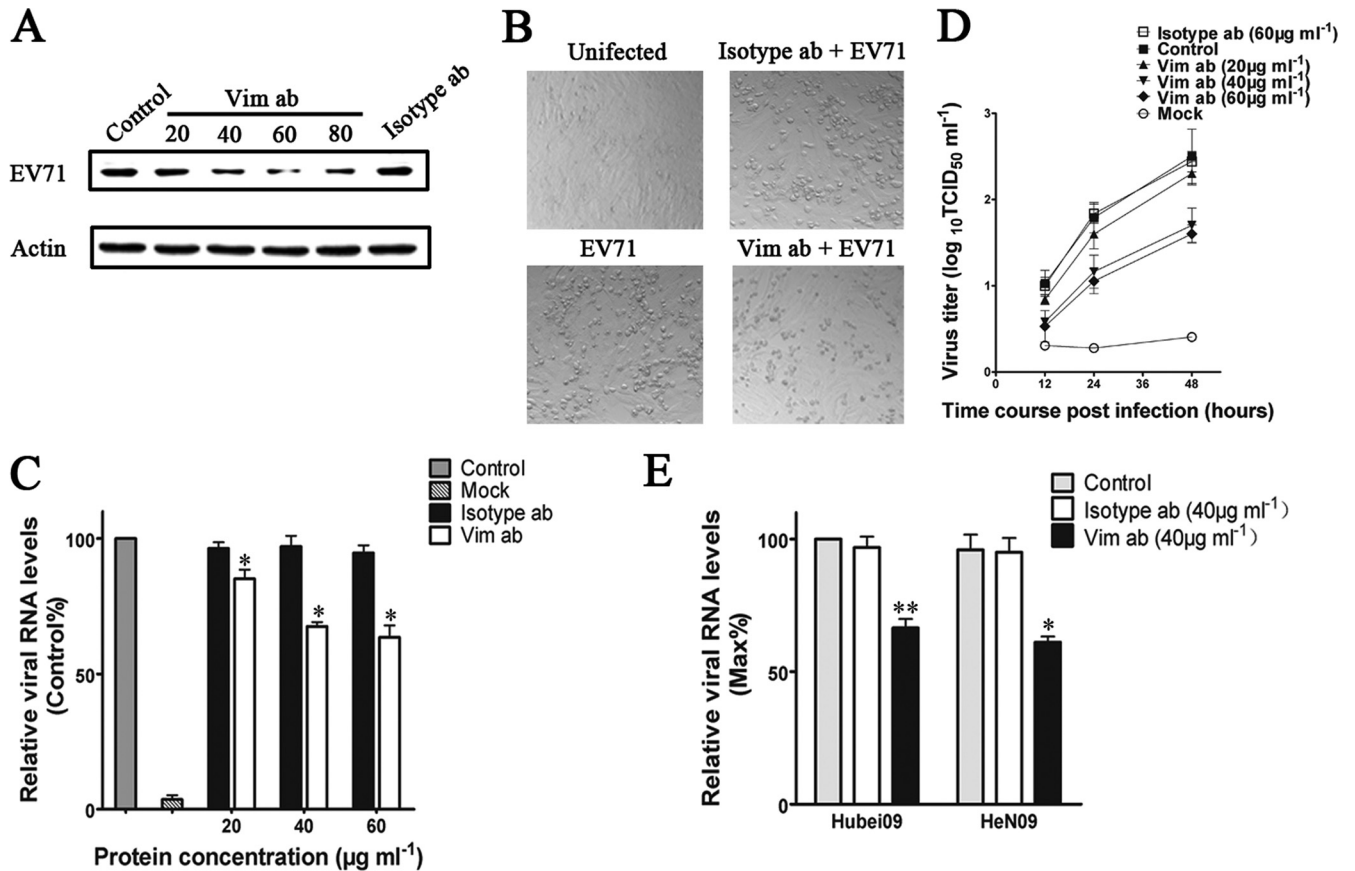
FIG 6 Effect of pretreating host cells with vimentin antibodies on the binding of EV71 to the cells. (A) Western blot analysis of EV71 BrCr replication in U251 cells that had been preincubated with vimentin antibodies prior to infection. Cells were pretreated with the indicated concentrations of vimentin antibodies (μg ml^{-1}) or rabbit IgG (isotype ab; 80 μg ml^{-1}) before being infected with EV71 for 1 h at 4°C. Cells were then lysed and subjected to Western blot analysis with antibody to EV71 and β-actin (internal control). Control, cells incubated with EV71. (B) CPE of EV71 BrCr infection viewed under a visible light phase microscope, showing representative fields of the uninfected control U251 cells (uninfected), vimentin antibody-pretreated cells infected with EV71 (Vim ab [60 μg ml^{-1}] and EV71), and rabbit IgG-pretreated cells infected with EV71 (isotype ab [60 μg ml^{-1}] and EV71). (C) Analysis of the binding of EV71 BrCr to U251 cells using quantitative RT-PCR. Cells were pretreated with vimentin antibodies (Vim ab; 60 μg ml^{-1}) or rabbit IgG (isotype ab; 60 μg ml^{-1}) before infection as described above. Control, untreated cells incubated with EV71; mock, incubated cells with no EV71; isotype ab, isotype antibody-pretreated cells infected with EV71; Vim, vimentin antibody-pretreated cells infected with EV71. (D) Graphs showing virus titers in infected U251 cells and the corresponding culture medium at 0, 12, and 24 h after infection. The cells were pretreated with vimentin antibody (Vim ab; 60 μg ml^{-1}) or rabbit IgG (isotype ab; 60 μg ml^{-1}) before infection. Control, untreated cells infected with EV71; mock, uninfected mock-treated cells. (E) Analysis of the influence of vimentin antibody (Vim ab) and isotype antibody (isotype ab) on the binding of EV71 Hubei09 and HeN09 strains to U251 cells using quantitative RT-PCR. Control, untreated cells incubated with EV71.

crease EV71 binding any further (Fig. 6C). At 24 h postinfection at 37°C, the vimentin antibody-pretreated U251 cells also suggested a reduction in virus replication compared to that of the IgG control, as demonstrated by a decrease in virus titers in the infected cell culture medium and lysates (Fig. 6D). To determine the effect of vimentin antibody pretreatment of cells on infection by other EV71 strains, U251 cells were pretreated with vimentin antibody as described above and then infected with EV71 Hunan 09 and HeN 09 for 1 h at 0°C. Analysis of cell surface-bound EV71 in these cells by quantitative PCR indicated a decrease in the amounts of EV71 Hunan 09 and HeN 09 virus binding to the U251 cells, implicating that vimentin was also involved in binding of other strains of EV71 to host cells (Fig. 6E). However, the inhibition effect of vimentin on the binding of EV71 Hunan 09 and BrCr strains to U251 cells appeared stronger than that in the HeN 09 strain.

A vimentin-knockdown cell line (VK-U251) with little vimentin expression was built using retrovirus-based RNA interference

(RNAi) vectors and was employed to verify the requirement of cell surface vimentin for the binding of EV71 to U251 cells. Flow cytometry analysis of vimentin expression on the cell surface of the knockdown line showed that the vimentin on the VK-U251 cell surface was present at a much lower level than in C-U251 and U251 cells (Fig. 7A). To analyze the effect of this decrease in vimentin expression on the binding of EV71 to the cell surface, VK-U251 and C-U251 cells were incubated with EV71 and subjected to flow cytometry 30 min later. The results (Fig. 7B) showed that a reduction in vimentin expression was accompanied by a dramatic decrease in virus binding in the VK-U251 cells compared to that in C-U251 and U251 cells. The same result was obtained when the amounts of virus binding to the cells were assessed by Western blotting and quantitative PCR analysis (Fig. 7C and D). As expected, inhibition of EV71 binding by vimentin antibody could not be detected in VK-U251 cells, as indicated by no reduction of EV71 RNA after vimentin antibody treatment (Fig. 7C). In addition, the replication of EV71 in VK-U251 cells was also re-
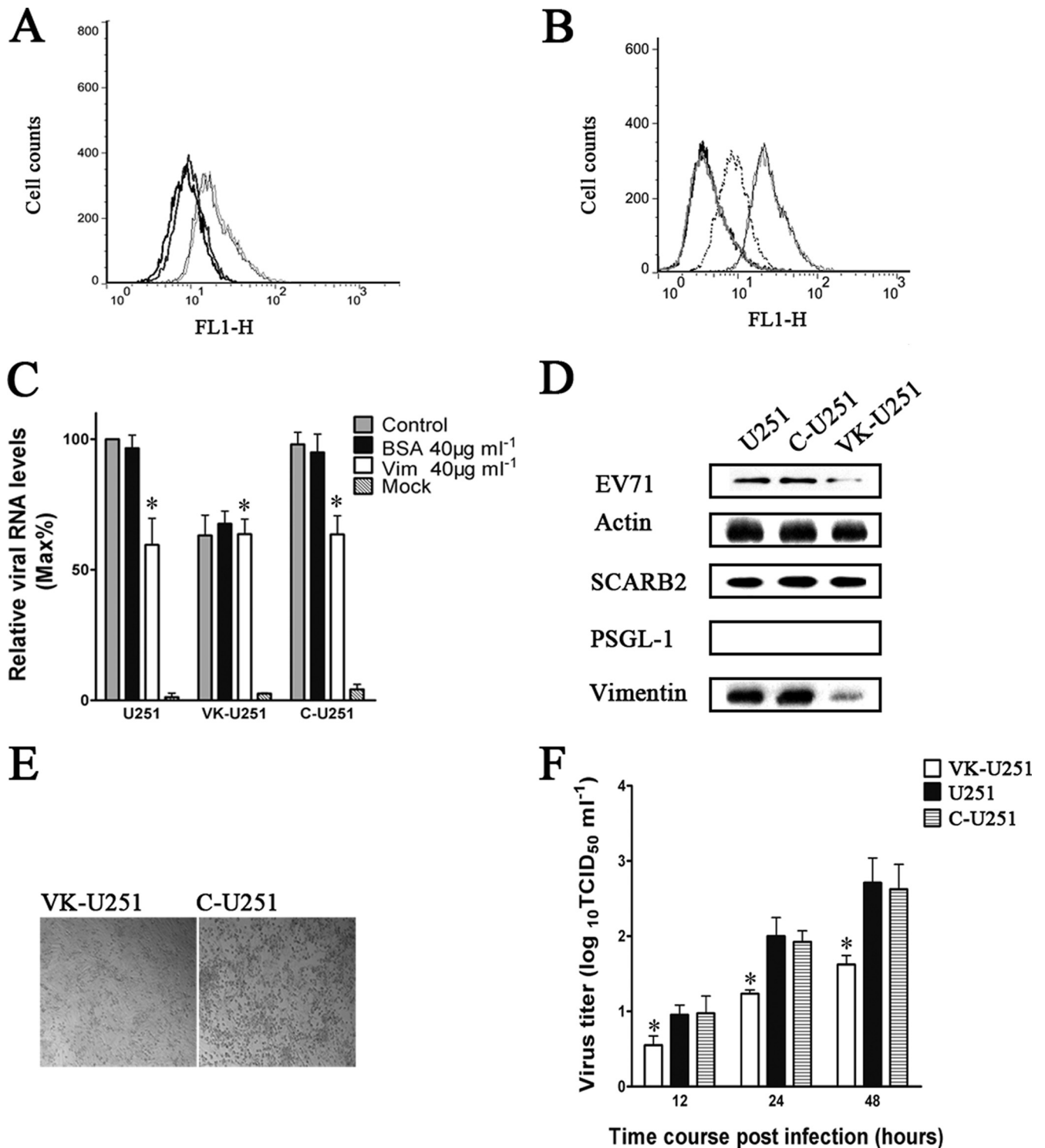
FIG 7 Effect of the downregulation of vimentin expression in U251 cells on the efficiency of EV71 binding and replication in host cells. U251, C-U251, and VK-U251 are cells with no vector, cells with empty vector, and cells with the vimentin knockdown plasmid, respectively. (A) Flow cytometry analysis of cell surface vimentin expression in U251 (gray hairline), C-U251 (black hairline), and VK-U251 (gray heavy line) cells. Nonpermeabilized cells were fixed and stained with antibody specific to vimentin and subjected to flow cytometry analysis. Thick black line, VK-U251 cells stained with mouse IgG. y axis (counts) = cell counts; x axis (FL1-H) = fluorescence density. (B) Flow cytometry analysis of the binding of EV71 to VK-U251 and C-U251 cells. VK-U251 and C-U251 cells were incubated with EV71 for 1 h at 4°C and then fixed, stained with antibody to EV71, and subjected to flow cytometry. Black heavy line, VK-U251 cells with no EV71 infection; gray heavy line, C-U251 cells with no EV71 infection; gray dotted line, infected VK-U251 cells stained with EV71 antibody; gray hairline, infected U251 cells stained with EV71 antibody; black hairline, infected C-U251 cells stained with EV71 antibody. (C) Analysis of EV71 binding in U251, VK-U251, and C-U251 cells that had been infected with virus inoculum preincubated with vimentin before transfection by quantitative RT-PCR. Control, cells incubated with untreated EV71; BSA, cells infected with virus inoculum preincubated with BSA; Vim, cells infected with virus inoculum preincubated with vimentin; mock, cells mock treated with no virus infection. (D) Western blot analysis of EV71 binding and expression of SCARB2, PSGL-1, and vimentin in U251, C-U251, and VK-U251 cells. The respective cells were infected with EV71 at 4°C for 1 h and then lysed and blotted with antibodies to either EV71, SCARB2, PSGL-1, vimentin, or β-actin (internal control). (E) Analysis of CPE of EV71 infection in C-U251 and VK-U251 cells after infection at 37°C for 48 h using a visible light phase microscope. (F) Determination of virus titers in infected U251, C-U251, and VK-U251 cells and the corresponding culture supernatants at 12, 24, and 48 h after infection with EV71.

duced, as shown by the presence of a relatively lower virus yield and an attenuation of the typical CPE found in cells with normal vimentin expression (Fig. 7E and F).

To investigate the interrelationships between vimentin and two previously identified EV71 cellular receptors, SCARB2 and PSGL-1, we first examined the cell surface SCARB2 and PSGL-1 in U251, HeLa, RD, Vero, and Jurkat cells. Flow cytometry analysis showed that U251, HeLa, RD, and Vero cells all expressed large amounts of SCARB2 on their cell surface (Fig. 8A), whereas only a small amount of SCARB2 was detected on the cell surface of Jurkat cells (Fig. 8A). Interestingly, no PSGL-1 could be detected on the U251, Vero, and HeLa cell surfaces (Fig. 8A). Conversely, Jurkat cells expressed large amounts of PSGL-1 on its cell surface (Fig. 8A). Further evidence suggested that SCARB2 might have relatively less influence on the binding of EV71 to U251 and VK-U251 cells, as only a small reduction of virus RNA levels was obtained from the cell surface of cells preincubated with SCARB2 antibody compared to that observed in cells preincubated with vimentin antibody (Fig. 8B). Moreover, SCARB2 antibody also had no influence on the blocking effect of vimentin antibody on EV71 binding in both U251 and VK-U251 cells (Fig. 8C). Strangely, an obvious decrease in virus yield was detected in U251 and VK-U251 cells pretreated with SCARB2 antibody (Fig. 8D and E), suggesting that SCARB2 may not be responsible for the initial binding between virus and host cells. In addition, pretreating cells with vimentin antibody did not affect the inhibition effect of SCARB2 antibody on EV71 binding. Pretreating cells with SCARB2 antibody also did not affect the inhibition effect of vimentin antibody on EV71 binding. These results indicated that EV71 binds to vimentin and SCARB2 at different sites.

Competitive inhibition assays with exogenous SCARB2 and vimentin were also done to investigate the effect of SCARB2 on EV71 and vimentin binding. EV71 particles were preincubated with vimentin, SCARB2, or BSA before being used to infect U251 cells. At 1 h postinfection at 0°C, samples of the cells were washed three times with culture medium and analyzed for bound virus particles by quantitative PCR. The results showed that there was a remarkable change (about 32% reduction) in the binding of EV71 in the vimentin-pretreated group compared to that of the BSA-treated or untreated group (Fig. 9A). However, pretreating the virus with SCARB2 had only a limited effect on EV71 binding, as reflected by no significant reduction of EV71 protein signals in this group (Fig. 9A). Analysis of EV71 replication in these samples at 24 h postinfection revealed that pretreatment of virus with SCARB2 resulted in a dramatic decrease of virus replication (Fig. 9B); however, the reduction in virus replication was less in the vimentin-preincubated group than in the SCARB2-treated group (Fig. 9B).

To determine whether the phenomenon described above was a unique feature of U251 cells or a feature common to other EV71-permissive cells, we investigated the inhibition of EV71 binding by SCARB2 and vimentin antibody in HeLa, Vero, and RD cells. These cell types were incubated with SCARB2 and vimentin antibody, and the binding of EV71 was analyzed by using quantitative PCR as described above. The results showed a dramatic reduction of EV71 RNA in the vimentin antibody-treated HeLa, Vero, and RD cells (Fig. 10A), while, as in the U251 cells, only a small amount of inhibition of EV71 binding was detected in the corresponding SCARB2 antibody-treated cells (Fig. 10A). In addition, an obvious decrease in virus yield was detected in the SCARB2

antibody-treated U251 cells (Fig. 10A). Pretreating cells with vimentin antibody also resulted in a reduction of virus yield in HeLa, Vero, and RD cells as well as U251 (Fig. 10B). Unexpectedly, the decrease in virus yield in the vimentin antibody-treated cells was less than that in the SCARB2 antibody-treated cells, implicating that the decrease in virus yield was not directly related to the reduction of virus binding. The effects of SCARB2 and vimentin antibody on the binding of EV71 Hunan 09 and HeN 09 strains to RD cells were also compared. Quantitative PCR analysis showed that pretreating cells with vimentin antibody also inhibited Hunan 09 and HeN 09 virus binding and replication in U251 cells (Fig. 10C), whereas pretreating cells with SCARB2 antibody did not influence the inhibition effect of vimentin antibody on the binding of these strains (Fig. 10C).

To investigate the role of host cell PSGL-1 on the binding of EV71 to cells, different permissive cell types were preincubated with PSGL-1 antibody (60 μg ml^{-1}) or isotype antibody (60 μg ml^{-1}) for 60 min at 4°C before being infected with EV71. At 1 h postinfection, virus particles bound to the cells were analyzed by quantitative PCR. Results showed that PSGL-1 antibody did not affect EV71 binding to U251, HeLa, Vero, and RD cells (Fig. 11A). However, preincubation of Jurkat cells with PSGL-1 antibody led to a dramatic reduction of EV71 binding in these cells (Fig. 11B). Moreover, pretreating Jurkat cells with vimentin antibody did not alter the effects of PSGL-1 antibody on EV71 binding (Fig. 11B), implicating that the sites of EV71 binding with PSGL-1 and vimentin are different. The virus yield in PSGL-1 antibody-treated Jurkat cells was also dramatically decreased compared to that of the IgG control group. The inhibition of EV71 infectivity by PSGL-1 antibody was not influenced by vimentin antibody (Fig. 11C).

It has been shown that certain mouse cells lines cannot efficiently support EV71 replication (50, 51). It is believed that mouse SCARB2 or PSGL-1 lacked the property required to mediate efficient EV71 infection (11, 52). The binding and replication of EV71 in mouse 3T3 cells was therefore studied. The results showed that the virus was able to bind to the 3T3 cell surface (Fig. 12A). Further analysis showed that 3T3 cells also have vimentin expressed on their cell surface (Fig. 12B), and vimentin antibody treatment of 3T3 cells also inhibited the binding of EV71 to the cells. In contrast, pretreating these cells with SCARB2 antibody or PSGL-1 antibody had no influence on EV71 binding (Fig. 12C). In addition, unlike human cell lines, 3T3 cells allowed only highly inefficient EV71 replication. Pretreating 3T3 cells with vimentin antibody also resulted in a reduction of virus yield (Fig. 12D). Coimmunoprecipitation was further performed to investigate the interaction between mouse vimentin and EV71 VP1. The results showed that a band corresponding to mouse vimentin could be detected in VP1-Flag protein eluate but not in control eluate (Fig. 12E), indicating that mouse vimentin could also interact with EV71 VP1. To further analyze the roles of mouse vimentin on EV71 binding, we performed EV71 binding experiments on 3T3 cells with reduced vimentin expression on their cell surface (produced by transfecting the cells with siRNA to vimentin) (Fig. 12F). We observed that a reduction of vimentin expression on the 3T3 cell surface was accompanied by a significant reduction in the binding of EV71 to the cells (Fig. 12G). These results indicated that the vimentin on the surface of mouse cells also contributed to virus-cell binding.

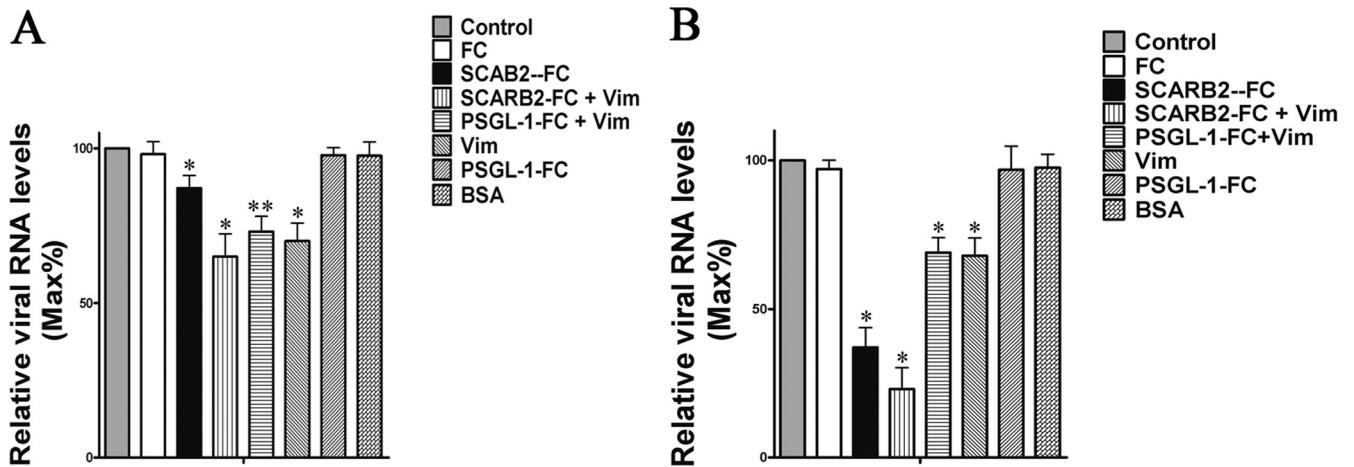To identify the domains responsible for VP1 and vimentin in-
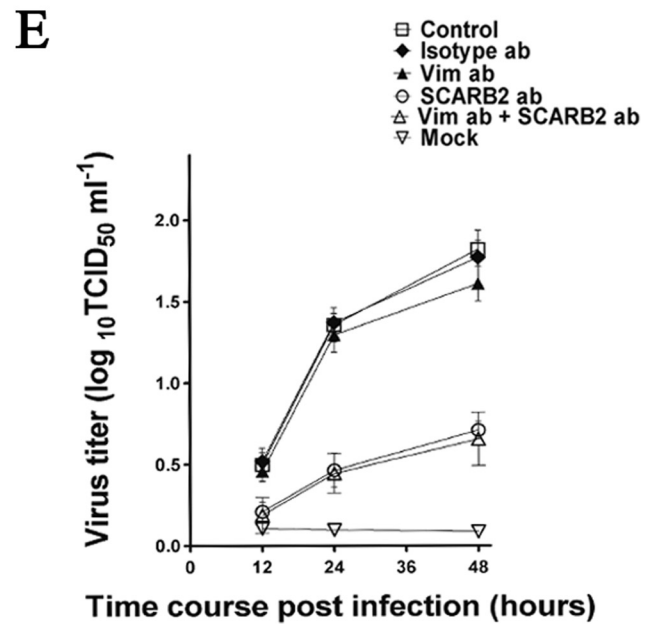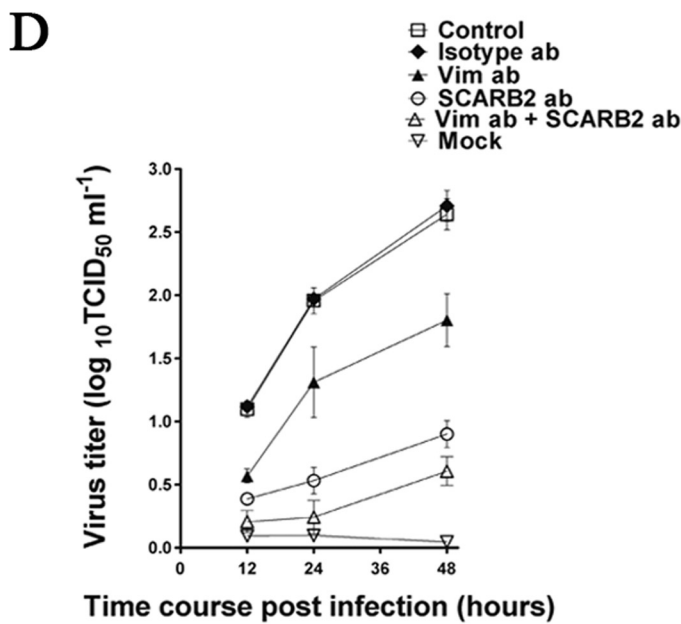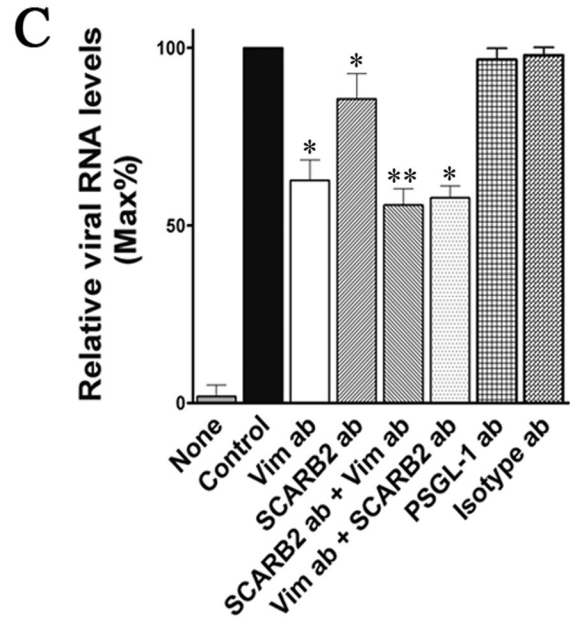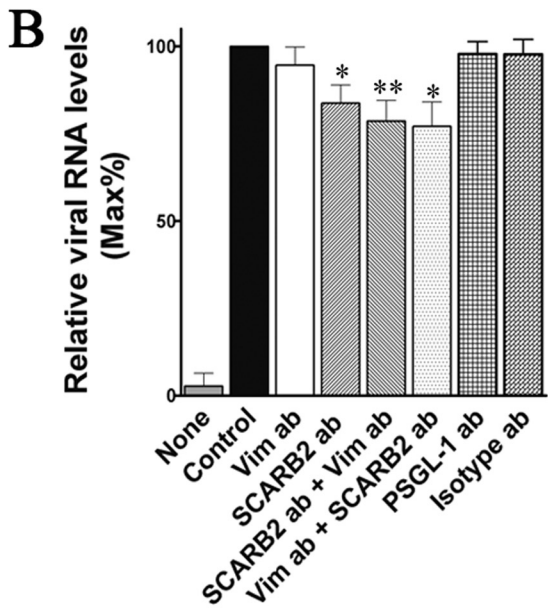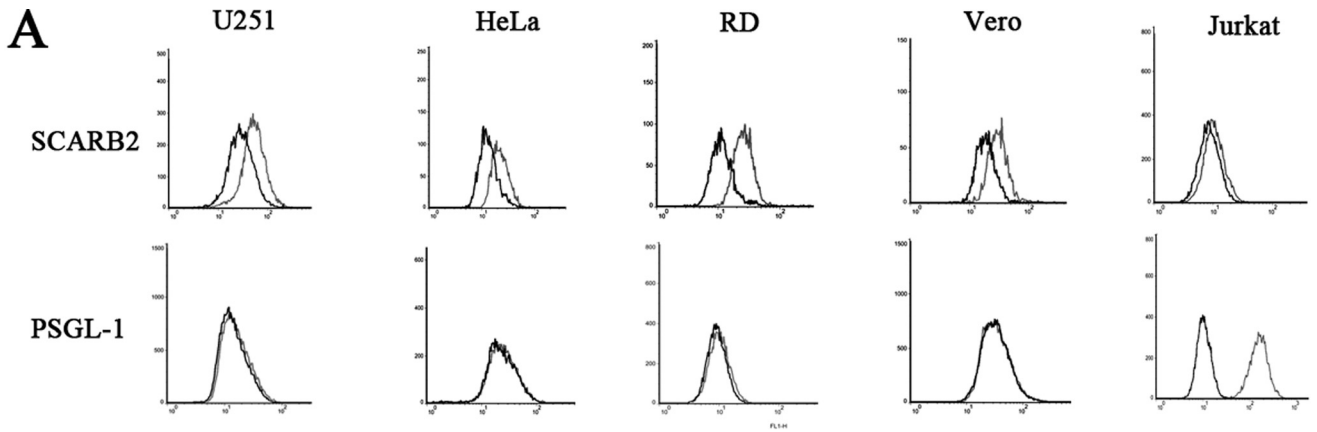
FIG 9 (A) Analysis of the binding of EV71 in U251 cells after pretreating the virus inoculum with BSA (20 µg ml^{-1}), mouse FC (20 µg ml^{-1}), PSGL-1-FC (20 µg ml^{-1}), SCARB2 (20 µg ml^{-1}), or/and vimentin (20 µg ml^{-1}) by using quantitative RT-PCR. Control, cells infected with EV71. (B) Virus titers in the supernatants and infected U251 cells after pretreating the virus inoculum with BSA (20 µg ml^{-1}), mouse FC (20 µg ml^{-1}), PSGL-1-FC (20 µg ml^{-1}), SCARB2 (20 µg ml^{-1}), or/and vimentin (20 µg ml^{-1}). Twenty-four hours postinfection, cells and supernatants were collected and frozen and thawed three times. After centrifugation for 10 min at 1,000 × *g*, the supernatants were recovered. A total of 200 µl of supernatants were used for the RNA extraction and quantitative PCR analysis. Mock, uninfected cells.

teraction, pulldown assays involving VP1 and vimentin truncates were performed. U251 cells were transfected with either full-length vimentin (aa 1 to 466), vimentin aa 1 to 230, vimentin aa 231 to 466, vimentin aa 1 to 115, vimentin aa 116 to 230, vimentin aa 1 to 56, or vimentin aa 57 to 115 and then lysed and incubated with either VP1-GST or GST, both precombined with glutathione agarose. The protein samples were then analyzed by Western blotting to detect for VP1 binding. The results showed that shortening the vimentin polypeptide from the N terminus that included aa 1 to 56 abolished the VP1 binding capacity of vimentin (Fig. 13A), suggesting that the N-terminal aa 1 to 56 of vimentin contained the domain directly responsible for the specific binding of EV71 VP1 to host cells. The role of the N-terminal vimentin aa 1 to 56 as an EV71-binding domain was further validated using functional assays in which all the vimentin truncates containing the N-terminal vimentin aa 1 to 56 tested were able to inhibit EV71 binding. The vimentin aa 1 to 56 truncate was also shown to be more effective in reducing virus yields than other vimentin truncates (Fig. 13B). Thus, these results implied that specific regions within vimentin aa 1 to 56 played a role in host-virus interactions that facilitates cell entry.

DISCUSSION

Specific interaction of virion constituents with cellular surface components is essential for infection of target cells by extracellular virus particles. For example, to initiate the infection process, interactions between virus particles and cell surface receptors mediate the initial attachment of the virus to the cell surface (53, 54). Vimentin is the major intermediate filament protein of astrocyte cells and is believed to be responsible for maintaining cell shape and integrity of the cytoplasm and stabilizing cytoskeletal interactions (55). It also plays a significant role in supporting and anchoring the nucleus, endoplasmic reticulum, and mitochondria. Its expression has been detected in cells of mesenchymal origin and is also present in cells adapted to tissue culture and many transformed cell lines (33). Several reports have suggested a conserved role for surface vimentin as a general attachment receptor for pathogen entry (34). However, it is still not clear how vimentin contributes to pathogen attachment and internalization. It is supposed that the interactions between vimentin and pathogens may increase the attachment of pathogens to the other cell surface molecules and subsequently enhances pathogen endocytosis. In this study, we have demonstrated that EV71 could attach to cell surface vimentin through VP1 and provided evidence that this interaction of EV71 with vimentin contributed to the establishment of EV71 infection since EV71 replication could be reduced by using either exogenous vimentin or an antibody against the cell surface vimentin. In addition, the decreased expression of vimentin on the cell surface resulted in a reduction of virus binding. Thus, our results

FIG 8 Effect of pretreating U251 cells with SCARB2 antibodies on the binding of EV71 to the cells. (A) Flow cytometry analysis of the cell surface expression of U251, RD, Vero, HeLa, and Jurkat cells. Cells were fixed and incubated with either mouse IgG (black line) or antibody to vimentin (gray line) and then incubated with the fluorescent secondary antibody and subjected to flow cytometry analysis. *y* axis (counts) = cell counts; *x* axis = fluorescence density. (B) Quantitative RT-PCR analysis of the binding of EV71 to VK-U251 cells that were infected after preincubation with antibodies to either vimentin (Vim ab; 60 µg ml^{-1}), PSGL-1 (PSGL-1 ab; 60 µg ml^{-1}), SCARB2 (SCARB2 ab; 60 µg ml^{-1}), or isotype IgG (isotype ab; 60 µg ml^{-1}). SCARB2 ab + Vim ab = cells preincubated with SCARB2 antibody (60 µg ml^{-1}) for 30 min at 37°C and then incubated with vimentin antibody for 30 min at 37°C. Vim ab + SCARB2 ab = cells preincubated with vimentin antibody for 30 min at 37°C followed by incubation with SCARB2 antibody for 30 min at 37°C. Control, EV71-infected cells without preincubation; mock, mock-treated cells with no virus. (C) Quantitative RT-PCR analysis of the binding of EV71 to U251 cells that were preincubated with antibodies to either vimentin, SCARB2, or isotype IgG as described above. (D) Determination of EV71 virus titers in infected U251 cells and the corresponding culture media at 12, 24, and 48 h after infection. The cells were preincubated with vimentin antibody (Vim ab; 60 µg ml^{-1}), SCARB2 antibody (SCARB2 ab; 60 µg ml^{-1}), or isotype IgG (control; 60 µg ml^{-1}) before infection. Mock, uninfected cells. (E) Determination of EV71 virus titers in infected VK-U251 cells and the corresponding culture supernatants as described for panel D. Cells were preincubated with vimentin antibody (Vim ab), SCARB2 antibody (SCARB2 ab), or isotype IgG (isotype ab) before infection. Control, EV71-infected cells without preincubation.
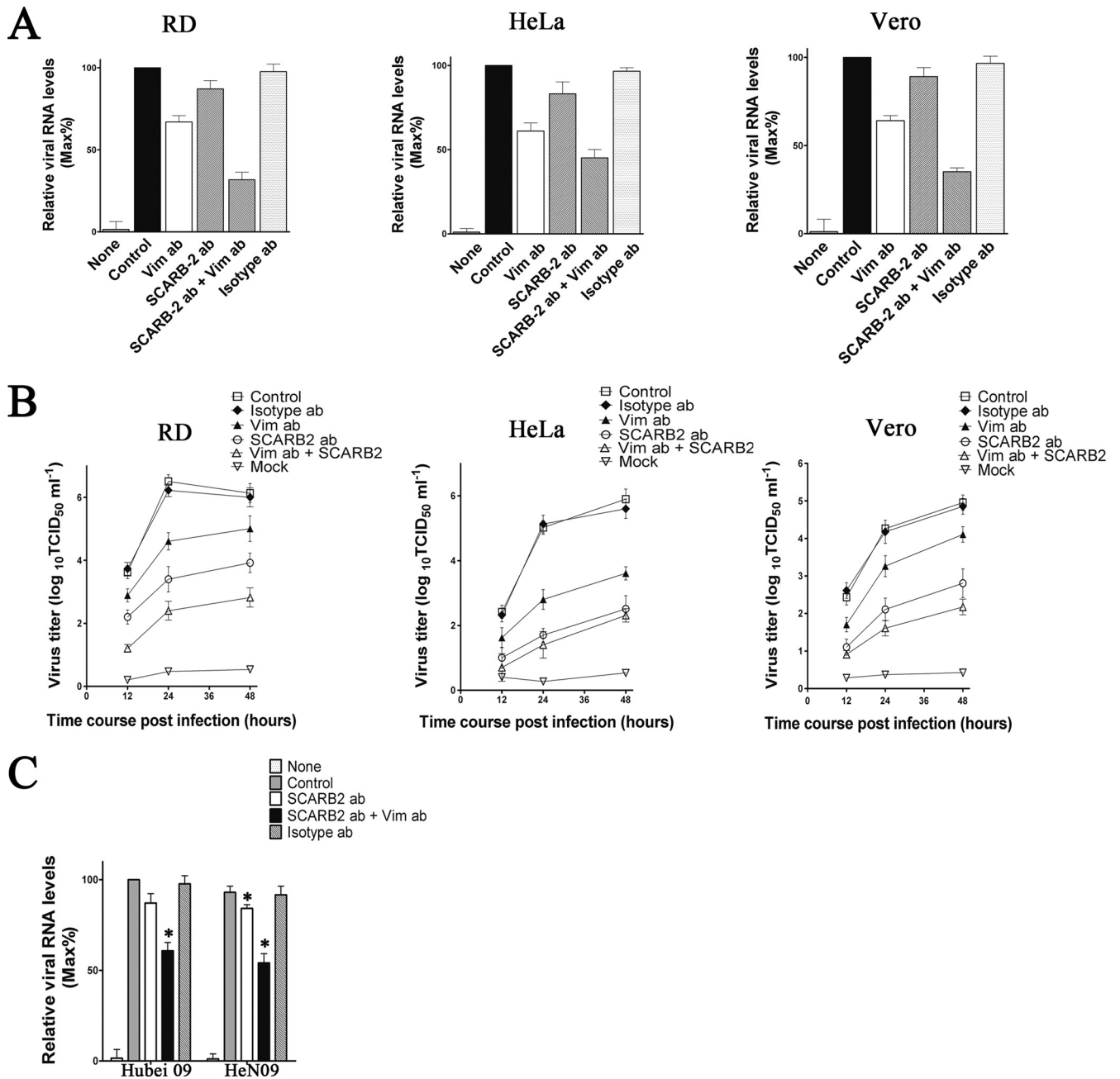
FIG 10 Effect of pretreating RD, HeLa, Vero, and Jurkat cells with SCARB2 antibodies on the binding of EV71 BrCr strain. (A) Quantitative RT-PCR analysis of the binding of EV71 to RD, HeLa, and Vero cells that were preincubated with antibodies to vimentin (Vim ab; 60 μg ml^{-1}), SCARB2 (SCARB2 ab; 60 μg ml^{-1}), or isotype IgG (isotype ab; 60 μg ml^{-1}). Control, EV71-infected cells without preincubation; mock, uninfected cells. (B) Determination of virus titers in EV71-infected RD, HeLa, and Vero cells and the corresponding culture supernatants. The cells were preincubated with vimentin antibody, SCARB2 antibody, or isotype IgG (control) before infection. (C) Quantitative RT-PCR analysis of the effect of pretreating U251 cells with SCARB2 antibodies (SCARB2 ab; 60 μg ml^{-1}) on the binding of EV71 Hubei 09 and HeN 09 strains to U251 cells. Control, EV71-infected cells with no preincubation; mock, uninfected cells.

indicated that vimentin expressed on the cell surface very likely serves as a capture receptor and acts as an attachment site for EV71. However, our results also suggested that the vimentin receptors could merely function as an additional route for virus entry into host cells, as virus infection was not completely eliminated by increasing the concentrations of vimentin antibody or exogenous vimentin. This suggests that cell surface vimentin is not essential for EV71 infection but helps the initial binding of virus to

host cells and that multiple receptors are involved during EV71 infection. Alternatively, the interaction of vimentin with EV71 VP1 might facilitate EV71 attachment to the other virus binding cellular receptors and subsequently enhance virus endocytosis into host cells.

SCARB2 and PSGL-1 have been reported to be the cellular receptors for EV71 (19, 20, 56). A comparison of the reported roles of SCARB2 and PSGL-1 in the virus infection process
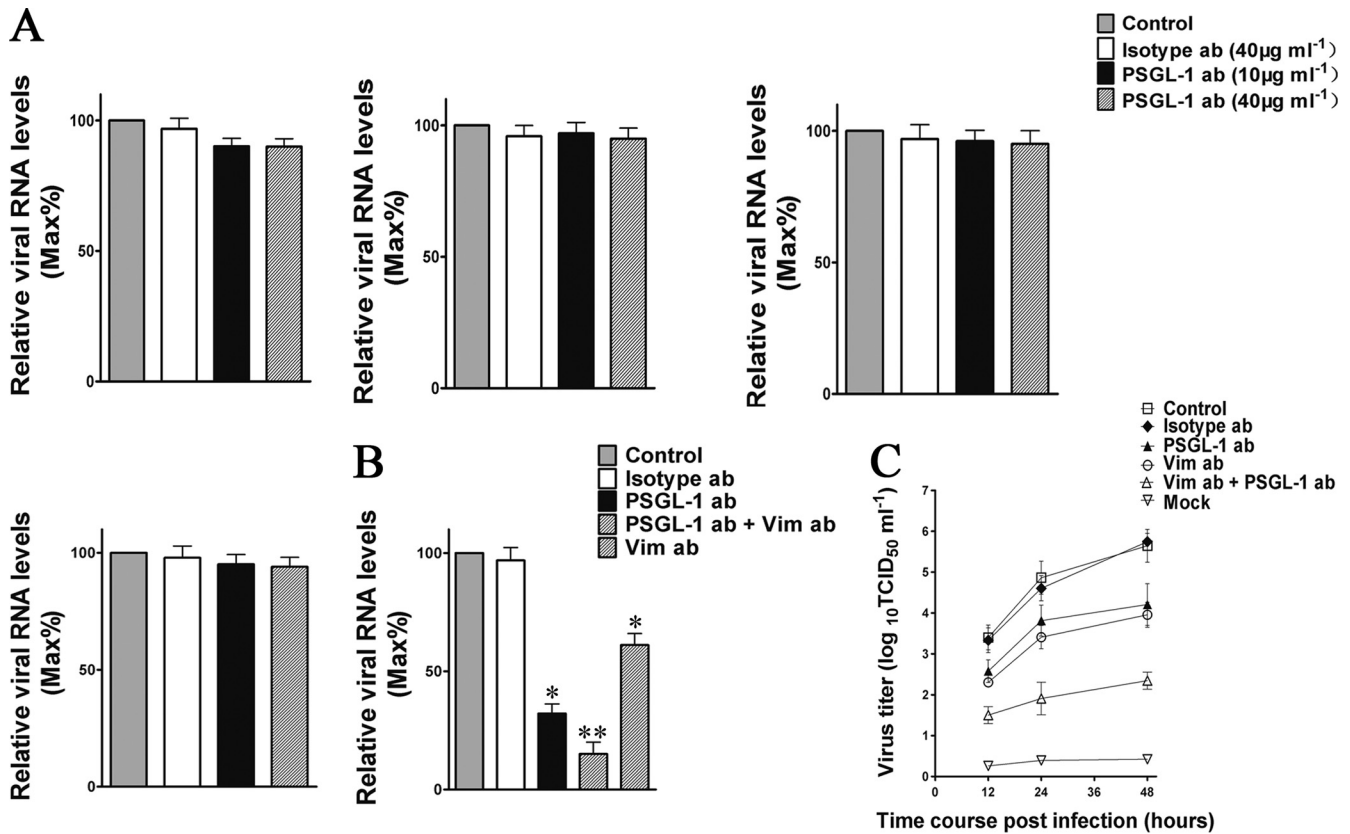
FIG 11 Experiments on the effect of pretreatment of RD, HeLa, Vero, and Jurkat cells with PSGL-1 antibodies on the binding of EV71 Hubei 09 strain. (A) Analysis of the binding of EV71 to RD, HeLa, and Vero cells preincubated with antibodies to vimentin, PSGL-1, or isotype IgG ($60 \mu g \, ml^{-1}$) by using quantitative RT-PCR as described in Materials and Methods. Control, cells infected with EV71. (B) Quantitative RT-PCR analysis of the effect of pretreatment of Jurkat cells with PSGL-1 antibodies on the binding of EV71. Control, cells infected with virus; mock, cells with no virus infection. (C) Virus titers in the supernatants and infected Jurkat cells that were preincubated with vimentin antibody, PSGL-1 antibody, or isotype IgG (control; $60 \mu g \, ml^{-1}$) before infection. The data are shown as mean virus titers ± SD based on three independent experiments.

showed that most EV71 strains were able to utilize SCARB2 as an entry receptor since all mouse cells that expressed human SCARB2 became susceptible to EV71 strains when tested (30). In contrast, mouse cells that expressed PSGL-1 were susceptible only to PSGL-1-binding strains (EV71-PB) and certain strains of CVA16 (30). In addition, cell surface expression of SCARB2 could be detected in most cell lines, while PSGL-1 expression could be detected only in myeloid cells and stimulated T lymphocytes (19). These reports are in accord with our observations that SCARB2, and not PSGL-1, could be detected on the cell surface of the nonleukocyte cell lines HeLa, Vero, U251, and RD. Although cell surface expression of PSGL-1 was observed in Jurkat T cells, in contrast, cell surface vimentin was expressed in all the cell lines tested. SCARB2 has been reported to play additional essential roles in the internalization and induction of virus uncoating, a step after virus attachment (57). Although numerous EV71 particles (a PB strain) were found binding to PSGL-1, this interaction did not induce conformational alterations in the cells (29). In addition, SCARB2 and PSGL-1 were reported to bind to different sites of the virion, and the affinity of the SCARB2-EV71 interaction was found to be different from that of the PSGL-1–EV71 interaction (30). In cells that expressed human SCARB2 and PSGL-1, EV71 was found to infect and spread more efficiently via SCARB2 than PSGL-1, despite that more virus particles had bound to L-PSGL-1 cells than to

L-SCARB2 cells (30). This result is consistent with our observation that pretreating cells with SCARB2 antibody had relatively less influence on virus binding compared to cells pretreated with vimentin antibody or PSGL-1 antibody. However, this observation was not in accord with our other observation that SCARB2 antibody pretreatment resulted in a dramatic decrease in virus titers compared to those of vimentin- and PSGL-1-pretreated cells. This implied that the amount of virus attaching to the cell surface might not solely determine the infection efficiency. Various reports suggest that vimentin may have roles in virus attachment and internalization but not in uncoating (34, 37). It is possible that the virus captured by PSGL-1 and vimentin could be uncoated either by SCARB2 in human cells that expressed these receptors or by other unknown molecules.

It is worth mentioning that the capacity for a virus to replicate is determined not only by the availability of host cell receptors and molecules that mediate virus entry but also by a host cell environment that favors virus gene replication, protein expression, and virus assembly and release. Several studies have indicated that mouse cells could not support robust EV71 infection (58–61). Other studies have shown that EV71 virion particles could attach to the surface of mouse L929 cells (28, 30), and low levels of virus replication can be detected in mouse L929 cells infected with EV71 (SK-EV006 and Nagoya strains) (20). This implies that, in oppo-
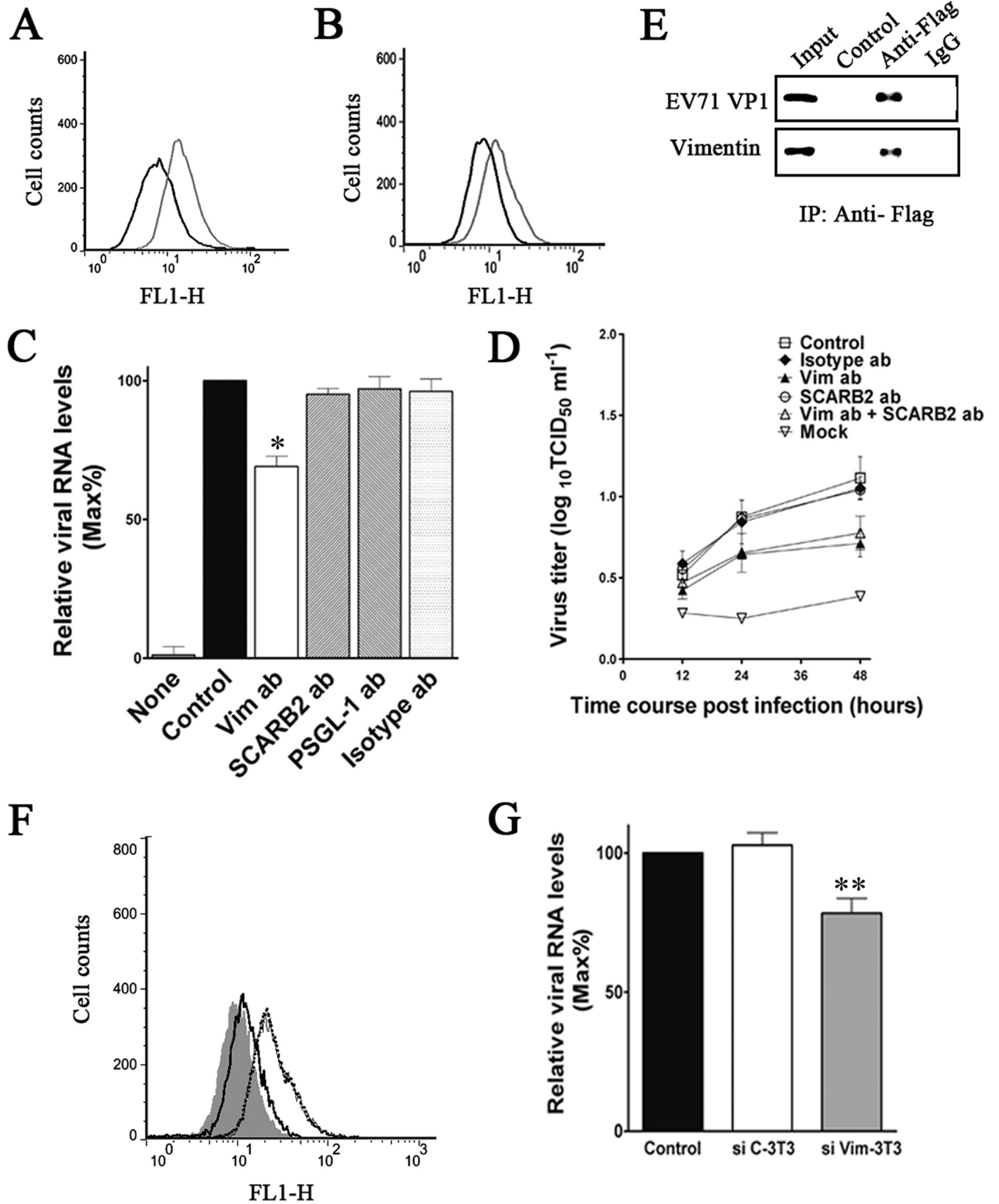
FIG 12 Analysis of the role of vimentin in EV71 binding in mouse 3T3 cells. (A) Detection of vimentin expression on the cell surface of mouse 3T3 cells. Cells were fixed and incubated with either mouse IgG (black line) or antibody to vimentin (gray line). The cells were then incubated with the fluorescent secondary antibody and subjected to flow cytometry analysis as described in Materials and Methods. y axis (counts) = cell counts; x axis = fluorescence density. (B) Flow cytometry analysis of the binding of EV71 to 3T3 cells. Cells were incubated with EV71 at an MOI of 20 at 4°C for 1 h, fixed, and incubated with either mouse IgG
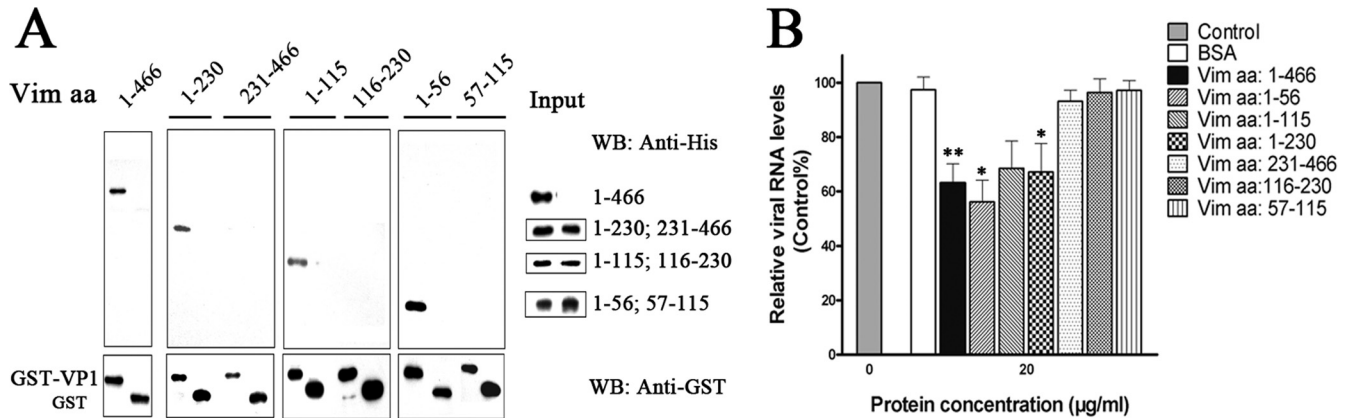
FIG 13 Identification of the domain of vimentin involved in the interaction with EV71 VP1. (A) Analysis of various truncated vimentin fragments for interaction with VP1. The His-tagged vimentin and its fragments (aa 1 to 466, 1 to 230, 231 to 466, 1 to 115, 116 to 230, 1 to 56, and 57 to 115) were subjected to a pulldown assay using the GST-VP1-coupled glutathione-Sepharose beads or GST beads as described in Materials and Methods. Proteins coprecipitating with the beads were analyzed by immunoblotting using anti-His antibody or anti-GST antibody. (B) Effect of pretreating EV71 inoculum with full-length vimentin and truncated vimentin on the binding of the virus to U251 cells. EV71 was pretreated with vimentin fragments at a concentration of 20 $\mu g\ ml^{-1}$ at 37°C for 1 h prior to infecting U251 cells. The cells were then infected with EV71 at 4°C for 1 h. Quantitative RT-PCR analysis was then performed to determine the EV71 RNA levels as described in Materials and Methods. Control, cells infected with untreated EV71.

sition to human SCARB2 and PSGL-1, other unspecified molecules on the surface of mouse cells might interact with EV71 and mediate its infection. One of these studies has also shown that infectious particles could be readily recovered from mouse cells transfected with EV71 genomic RNA (20), suggesting that the restriction of EV71 infection in mouse cells probably occurred at one of the early steps of infection and that mouse cells might lack the cell receptors essential for productive infection. However, in our study, we have observed that EV71 could bind to mouse 3T3 cells by interacting with cell surface vimentin, leading to a very limited replication of EV71 in 3T3 cells. In addition, a reduction of vimentin expression on the 3T3 cell surface did result in a decrease in the binding of virus particles to the cells. Thus, the low efficiency of EV71 infection and replication in mouse cells might not be due to a lack of attachment receptors but attributed mainly to an absence or low expression of essential cell receptors that mediate virus internalization, endocytosis, and/or uncoating. Furthermore, it is unlikely that mouse SCARB2 and PSGL-1 are involved in virus-cell interaction since pretreating 3T3 cells with SCARB2 and PSGL-1 antibody did not decrease EV71 binding to these cells. This suggests that mouse cells could possess other molecules that lead to very limited infection.

We have found that vimentin mediated the interaction between vimentin and VP1. Dramatic decreases in virus binding and virus yields were observed in cells pretreated with vimentin fragments that contained the N-terminal amino acids 1 to 56 of vi-

mentin. A vimentin monomer, like all other intermediate filaments, has a central α-helical domain, capped at each end by a nonhelical amino (head) and carboxyl (tail) domain (62). Two vimentin molecules form a coiled-coil dimer that is the basic subunit of vimentin assembly (63, 64). Thus, we can envisage that the head domains of the cell surface vimentin interact with EV71 VP1 and increase the attachment of EV71 to host cells. In contrast, it was demonstrated that the binding of SCARB2 to EV71 occurred within the luminal domain of SCARB2 at amino acids 142 to 204 and that amino acids 144 to 151 were particularly important (28). It has been shown that EV71 VP2 could participate in EV71–PSGL-1 binding (50). In our study, we have found that EV71 might bind with vimentin at a different site than for SCARB2 or PSGL-1 since vimentin binding did not influence the interaction between EV71 and SCARB2 or PSGL-1. In addition, the virus-vimentin interaction was shown to be common to other selected C4 genotypes of EV71, suggesting that the interaction with vimentin could be a common feature of most, if not all, of the circulating EV71 viruses. In consideration of the broad distribution of vimentin in animal tissues, we hypothesize that vimentin might contribute to the proliferation of virus infection by broadening the target cells *in vivo*. Moreover, it might also be more than an attachment site on the host cell surface.

In conclusion, we believe this study delivers important findings on the roles of vimentin filaments in relation to EV71 infection. This work provides information that not only improves our un-

(black line) or antibody to EV71 (gray line). (C) Quantitative RT-PCR analysis of the binding of EV71 to 3T3 cells that were preincubated with antibodies to vimentin, SCARB2, PSGL-1, or isotype IgG (60 $\mu g\ ml^{-1}$) and then infected with EV71. Control, EV71-infected cells without preincubation; mock, uninfected cells. (D) Determination of virus titers in EV71-infected 3T3 cells and the corresponding culture supernatants at 12, 24, and 48 h postinfection. The cells were preincubated with vimentin antibody, SCARB2 antibody, or isotype IgG (control) before infection. Mock, uninfected cells. (E) Coimmunoprecipitation and Western blot analysis of the interaction between mouse vimentin and EV71 VP1 as described in Materials and Methods. 3T3 cells were transfected with plasmids expressing VP1. Coimmunoprecipitation was performed with Flag antibody. The precipitated proteins were analyzed by Western blotting using antibodies to vimentin 1 and Flag. Control, proteins from cell lysate incubated with agarose beads; VP1, proteins from cell lysate incubated with Flag-conjugated agarose beads; IgG, proteins from cell lysate incubated with IgG-conjugated agarose beads. (F) Detection of vimentin expression on the cell surface of mouse 3T3 (black dotted line), siC-3T3 (gray line), and siVim-3T3 (black line) cells. Cells were fixed and incubated with either mouse IgG (shaded area) or antibody to vimentin. The cells were then incubated with the fluorescent secondary antibody and subjected to flow cytometry analysis as described in Materials and Methods. (G) Analysis of the binding of EV71 to 3T3, siC-3T3, and siVim-3T3 cells using quantitative RT-PCR.

derstanding of EV71 pathogenesis but also presents us with potential new strategies for the treatment of diseases caused by EV71 infections. For example, it might be possible to develop some antibodies, peptides, or small compounds for the prevention and/or treatment of EV71 infections by blocking the binding between EV71 and vimentin. However, the functional significance of vimentin-EV71 interaction during the natural infection process of these important human viruses remains to be elucidated.

REFERENCES

1. **Hagiwara A, Tagaya I, Yoneyama T.** 1978. Epidemic of hand, foot and mouth disease associated with enterovirus-71 infection. Intervirology **9**:60–63. http://dx.doi.org/10.1159/000148922.
2. **Ooi MH, Wong SC, Lewthwaite P, Cardosa MJ, Solomon T.** 2010. Clinical features, diagnosis, and management of enterovirus 71. Lancet Neurol. **9**:1097–1105. http://dx.doi.org/10.1016/S1474-4422(10)70209-X.
3. **Solomon T, Lewthwaite P, Perera D, Cardoso MJ, McMinn P, Ooi MH.** 2010. Virology, epidemiology, pathogenesis, and control of enterovirus 71. Lancet Infect. Dis. **10**:778–790. http://dx.doi.org/10.1016/S1473-3099(10)70194-8.
4. **Tagaya I, Takayama R, Hagiwara A.** 1981. A large-scale epidemic of hand, foot and mouth disease associated with enterovirus-71 infection in Japan in 1978. Jpn. J. Med. Sci. Biol. **34**:191–196.
5. **Chan LG, Parashar UD, Lye MS, Ong FGL, Zaki SR, Alexander JP, Ho KK, Han LL, Pallansch MA, Suleiman AB, Jegathesan M, Anderson LJ, Grp OS.** 2000. Deaths of children during an outbreak of hand, foot, and mouth disease in Sarawak, Malaysia: clinical and pathological characteristics of the disease. Clin. Infect. Dis. **31**:678–683. http://dx.doi.org/10.1086/314032.
6. **Ho MT, Chen ER, Hsu KH, Twu SJ, Chen KT, Tsai SF, Wang JR, Shih SR, Taiwan Enterovirus Epidemic Working Group.** 1999. An epidemic of enterovirus 71 infection in Taiwan. N. Engl. J. Med. **341**:929–935. http://dx.doi.org/10.1056/NEJM199909233411301.
7. **Wu Y, Yeo A, Phoon MC, Tan EL, Poh CL, Quak SH, Chow VTK.** 2010. The largest outbreak of hand, foot and mouth disease in Singapore in 2008: the role of enterovirus 71 and coxsackievirus A strains. Int. J. Infect. Dis. **14**:E1076–E1081. http://dx.doi.org/10.1016/j.ijid.2010.07.006.
8. **Qiu J.** 2008. Enterovirus 71 infection: a new threat to global public health? Lancet Neurol. **7**:868–869. http://dx.doi.org/10.1016/S1474-4422(08)70207-2.
9. **Goh KT, Doraisingham S, Tan JL, Lim GN, Chew SE.** 1982. An outbreak of hand, foot, and mouth disease in Singapore. B World Health Organ. **60**:965–969.
10. **Huang CC, Liu CC, Chang YC, Chen CY, Wang ST, Yeh TF.** 1999. Neurologic complications in children with enterovirus 71 infection. N. Engl. J. Med. **341**:936–942. http://dx.doi.org/10.1056/NEJM199909233411302.
11. **Khong WX, Yan B, Yeo HM, Tan EL, Lee JJ, Ng JKW, Chow VT, Alonso S.** 2012. A non-mouse-adapted enterovirus 71 (EV71) strain exhibits neurotropism, causing neurological manifestations in a novel mouse model of EV71 infection. J. Virol. **86**:2121–2131. http://dx.doi.org/10.1128/JVI.06103-11.
12. **Lee MS, Lin TY, Chiang PS, Li WC, Luo ST, Tsao KC, Liou GY, Huang ML, Hsia SH, Huang YC, Chang SC.** 2010. An investigation of epidemic enterovirus 71 infection in Taiwan, 2008 clinical, virologic, and serologic

features. Pediatr. Infect. Dis. J. **29**:1030–1034. http://dx.doi.org/10.1097/INF.0b013e3181e52945.
13. **Lum LCS, Wong KT, Lam SK, Chua KB, Goh AYT.** 1998. Neurogenic pulmonary oedema and enterovirus 71 encephalomyelitis. Lancet **352**:1391. http://dx.doi.org/10.1016/S0140-6736(05)60789-1.
14. **Lin YW, Chang KC, Kao CM, Chang SP, Tung YY, Chen SH.** 2009. Lymphocyte and antibody responses reduce enterovirus 71 lethality in mice by decreasing tissue viral loads. J. Virol. **83**:6477–6483. http://dx.doi.org/10.1128/JVI.00434-09.
15. **Lu J, Yi LN, Zhao J, Yu J, Chen Y, Lin MC, Kung HF, He ML.** 2012. Enterovirus 71 disrupts interferon signaling by reducing the level of interferon receptor 1. J. Virol. **86**:3767–3776. http://dx.doi.org/10.1128/JVI.06687-11.
16. **Chang L, Huang L, Gau SS, Wu Y, Hsia S, Fan T, Lin K, Huang Y, Lu C, Lin T.** 2007. Neurodevelopment and cognition in children after enterovirus 71 infection. N. Engl. J. Med. **356**:1226–1234. http://dx.doi.org/10.1056/NEJMoa065954.
17. **Huang CC, Liu CC, Chang YC.** 2000. Enterovirus 71 infection and neurologic complications. Reply. N. Engl. J. Med. **342**:357–358. http://dx.doi.org/10.1056/NEJM199909233411302.
18. **Hussain KM, Leong KLJ, Ng MML, Chu JJH.** 2011. The essential role of cathrin-mediated endocytosis in the infectious entry of human enterovirus 71. J. Biol. Chem. **286**:309–321. http://dx.doi.org/10.1074/jbc.M110.168468.
19. **Nishimura Y, Shimojima M, Tano Y, Miyamura T, Wakita T, Shimizu H.** 2009. Human P-selectin glycoprotein ligand-1 is a functional receptor for enterovirus 71. Nat. Med. **15**:794–797. http://dx.doi.org/10.1038/nm.1961.
20. **Yamayoshi S, Yamashita Y, Li JF, Hanagata N, Minowa T, Takemura T, Koike S.** 2009. Scavenger receptor B2 is a cellular receptor for enterovirus 71. Nat. Med. **15**:798–801. http://dx.doi.org/10.1038/nm.1992.
21. **Davenpeck KL, Brummet ME, Hudson SA, Mayer RJ, Bochner BS.** 2000. Activation of human leukocytes reduces surface P-selectin glycoprotein ligand-1 (PSGL-1, CD162) and adhesion to P-selectin *in vitro*. J. Immunol. **165**:2764–2772.
22. **Lim YC, Snapp K, Kansas GS, Camphausen R, Ding H, Luscinskas FW.** 1998. Important contributions of P-selectin glycoprotein ligand-1-mediated secondary capture to human monocyte adhesion to P-selectin, E-selectin, and TNF-alpha-activated endothelium under flow *in vitro*. J. Immunol. **161**:2501–2508.
23. **Ma YQ, Plow EF, Geng JG.** 2004. P-selectin binding to P-selectin glycoprotein ligand-1 induces an intermediate state of alpha M beta 2 activation and acts cooperatively with extracellular stimuli to support maximal adhesion of human neutrophils. Blood **104**:2549–2556. http://dx.doi.org/10.1182/blood-2004-03-1108.
24. **Nishimura Y, Wakita T, Shimizu H.** 2010. Tyrosine sulfation of the amino terminus of PSGL-1 is critical for enterovirus 71 infection. PLoS Pathog. **66**:e1001174. http://dx.doi.org/10.1371/journal.ppat.1001174.
25. **Crombie R, Silverstein R.** 1998. Lysosomal integral membrane protein II binds thrombospondin-1: structure-function homology with the cell adhesion molecule CD36 defines a conserved recognition motif. J. Biol. Chem. **273**:4855–4863. http://dx.doi.org/10.1074/jbc.273.9.4855.
26. **Vega MA, Rodriguez F, Segui B, Cales C, Alcalde J, Sandoval IV.** 1991. Targeting of lysosomal integral membrane-protein Limp-Ii—the tyrosine-lacking carboxyl cytoplasmic tail of Limp-Ii is sufficient for direct targeting to lysosomes. J. Biol. Chem. **266**:16269–16272.
27. **Eskelinen EL, Tanaka Y, Saftig P.** 2003. At the acidic edge: emerging functions for lysosomal membrane proteins. Trends Cell Biol. **13**:137–145. http://dx.doi.org/10.1016/S0962-8924(03)00005-9.
28. **Chen P, Song ZL, Qi YH, Feng XF, Xu NQ, Sun YY, Wu X, Yao X, Mao QY, Li XL, Dong WJ, Wan XB, Huang N, Shen XL, Liang ZL, Li WH.** 2012. Molecular determinants of enterovirus 71 viral entry cleft around Gln-172 on Vp1 protein interacts with variable region on scavenge receptor B2. J. Biol. Chem. **287**:6406–6420. http://dx.doi.org/10.1074/jbc.M111.301622.
29. **Yamayoshi S, Iizuka S, Yamashita T, Minagawa H, Mizuta K, Okamoto M, Nishimura H, Sanjoh K, Katsushima N, Itagaki T, Nagai Y, Fujii K, Koike S.** 2012. Human SCARB2-dependent infection by coxsackievirus A7, A14, and A16 and enterovirus 71. J. Virol. **86**:5686–5696. http://dx.doi.org/10.1128/JVI.00020-12.
30. **Yamayoshi S, Ohka S, Fujii K, Koike S.** 2013. Functional Comparison of SCARB2 and PSGL1 as receptors for enterovirus 71. J. Virol. **87**:3335–3347. http://dx.doi.org/10.1128/JVI.02070-12.

31. **Yang B, Chuang H, Yang KD.** 2009. Sialylated glycans as receptor and inhibitor of enterovirus 71 infection to DLD-1 intestinal cells. Virol. J. **6:**141. http://dx.doi.org/10.1186/1743-422X-6-141.

32. **Yang SL, Chou YT, Wu CN, Ho MS.** 2011. Annexin II binds to capsid protein VP1 of enterovirus 71 and enhances viral infectivity. J. Virol. **85:** 11809–11820. http://dx.doi.org/10.1128/JVI.00297-11.

33. **Goldman RD, Khuon S, Chou YH, Opal P, Steinert PM.** 1996. The function of intermediate filaments in cell shape and cytoskeletal integrity. J. Cell Biol. **134:**971–983. http://dx.doi.org/10.1083/jcb.134.4.971.

34. **Das S, Ravi V, Desai A.** 2011. Japanese encephalitis virus interacts with vimentin to facilitate its entry into porcine kidney cell line. Virus Res. **160:**404–408. http://dx.doi.org/10.1016/j.virusres.2011.06.001.

35. **Kim JK, Fahad AM, Shanmukhappa K, Kapil S.** 2006. Defining the cellular target (s) of porcine reproductive and respiratory syndrome virus blocking monoclonal antibody 7G10. J. Virol. **80:**689–696. http://dx.doi.org/10.1128/JVI.80.2.689-696.2006.

36. **Klimstra WB, Ryman KD, Johnston RE.** 1998. Adaptation of sindbis virus to BHK cells selects for use of heparan sulfate as an attachment receptor. J. Virol. **72:**7357–7366.

37. **Koudelka KJ, Destito G, Plummer EM, Trauger SA, Siuzdak G, Manchester M.** 2009. Endothelial targeting of cowpea mosaic virus (CPMV) via surface vimentin. PLoS Pathog. **5:**e1000417. http://dx.doi.org/10.1371/journal.ppat.1000417.

38. **Lee WC, Fuller AO.** 1993. Herpes-simplex virus type-1 and pseudorabies virus bind to a common saturable receptor on Vero cells that is not heparan-sulfate. J. Virol. **67:**5088–5097.

39. **Nedellec P, Vicart P, Laurent-Winter C, Martinat C, Prevost MC, Brahic M.** 1998. Interaction of Theiler's virus with intermediate filaments of infected cells. J. Virol. **72:**9553–9560.

40. **Cui S, Wang J, Fan TT, Qin B, Guo L, Lei XB, Wang JW, Wang MT, Jin Q.** 2011. Crystal structure of human enterovirus 71 3C protease. J. Mol. Biol. **408:**449–461. http://dx.doi.org/10.1016/j.jmb.2011.03.007.

41. **Foo DGW, Alonso S, Chow VTK, Poh CL.** 2007. Passive protection against lethal enterovirus 71 infection in newborn mice by neutralizing antibodies elicited by a synthetic peptide. Microbes Infect. **9:**1299–1306. http://dx.doi.org/10.1016/j.micinf.2007.06.002.

42. **Luca VC, AbiMansour J, Nelson CA, Fremont DH.** 2012. Crystal structure of the Japanese encephalitis virus envelope protein. J. Virol. **86:**2337–2346. http://dx.doi.org/10.1128/JVI.06072-11.

43. **Kim H, Nakamura F, Lee W, Shifrin Y, Arora P, McCulloch CA.** 2010. Filamin A is required for vimentin-mediated cell adhesion and spreading. Am. J. Physiol. Cell Physiol. **298:**C221–C236. http://dx.doi.org/10.1152/ajpcell.00323.2009.

44. **Ermakova S, Choi BY, Choi HS, Kang BS, Bode AM, Dong ZG.** 2005. The intermediate filament protein vimentin is a new target for epigallocatechin gallate. J. Biol. Chem. **280:**16882–16890. http://dx.doi.org/10.1074/jbc.M414185200.

45. **Liu CC, Guo MS, Lin FHY, Hsiao KN, Chang KHW, Chou AH, Wang YC, Chen YC, Yang CS, Chong PCS.** 2011. Purification and characterization of enterovirus 71 viral particles produced from Vero cells grown in a serum-free microcarrier bioreactor system. PLoS One **6:**e20005. http://dx.doi.org/10.1371/journal.pone.0020005.

46. **Cong HL, Jiang Y, Tien P.** 2011. Identification of the myelin oligodendrocyte glycoprotein as a cellular receptor for rubella virus. J. Virol. **85:** 11038–11047. http://dx.doi.org/10.1128/JVI.05398-11.

47. **Wang B, Xi XY, Lei XB, Zhang XY, Cui S, Wang JW, Jin Q, Zhao ZD.** 2013. Enterovirus 71 protease 2A(pro) targets MAVS to inhibit anti-viral type I interferon responses. PLoS Pathog. **9:**e1003231. http://dx.doi.org/10.1371/journal.ppat.1003231.

48. **Yang Z, Li GD, Zhang YQ, Liu XM, Tien P.** 2012. A novel minicircle vector based system for inhibiting the replication and gene expression of enterovirus 71 and coxsackievirus A16. Antiviral Res. **96:**234–244. http://dx.doi.org/10.1016/j.antiviral.2012.08.003.

49. **Plevka P, Perera R, Yap ML, Cardosa J, Kuhn RJ, Rossmann MG.** 2013. Structure of human enterovirus 71 in complex with a capsid-binding inhibitor. Proc. Nat. Acad. Sci. U. S. A. **110:**5463–5467. http://dx.doi.org/10.1073/pnas.1222379110.

50. **Miyamura K, Nishimura Y, Abo M, Wakita T, Shimizu H.** 2011. Adaptive mutations in the genomes of enterovirus 71 strains following infection of mouse cells expressing human P-selectin glycoprotein ligand-1. J. Gen. Virol. **92:**287–291. http://dx.doi.org/10.1099/vir.0.022418-0.

51. **Zaini Z, Phuektes P, McMinn P.** 2012. Mouse adaptation of a subgenogroup B5 strain of human enterovirus 71 is associated with a novel lysine to glutamic acid substitution at position 244 in protein VP1. Virus Res. **167:**86–96. http://dx.doi.org/10.1016/j.virusres.2012.04.009.

52. **Huang SW, Wang YF, Yu CK, Su IJ, Wang JR.** 2012. Mutations in VP2 and VP1 capsid proteins increase infectivity and mouse lethality of enterovirus 71 by virus binding and RNA accumulation enhancement. Virology **422:**132–143. http://dx.doi.org/10.1016/j.virol.2011.10.015.

53. **Mettenleiter TC.** 2002. Brief overview on cellular virus receptors. Virus Res. **82:**3–8. http://dx.doi.org/10.1016/S0168-1702(01)00380-X.

54. **Schneider-Schaulies J.** 2000. Cellular receptors for viruses: links to tropism and pathogenesis. J. Gen. Virol. **81:**1413–1429.

55. **Nieminen M, Henttinen T, Merinen M, Marttila-Ichihara F, Eriksson JE, Jalkanen S.** 2006. Vimentin function in lymphocyte adhesion and transcellular migration. Nat. Cell Biol. **8:**156–162. http://dx.doi.org/10.1038/ncb1355.

56. **Lin YW, Lin HY, Tsou YL, Chitra E, Hsiao KN, Shao HY, Liu CC, Sia C, Chong P, Chow YH.** 2012. Human SCARB2-mediated entry and endocytosis of EV71. PLoS One **7:**e30507. http://dx.doi.org/10.1371/journal.pone.0030507.

57. **Yamayoshi S, Koike S.** 2011. Identification of a human SCARB2 region that is important for enterovirus 71 binding and infection. J. Virol. **85:** 4937–4946. http://dx.doi.org/10.1128/JVI.02358-10.

58. **Arita M, Ami Y, Wakita T, Shimizu H.** 2008. Cooperative effect of the attenuation determinants derived from poliovirus Sabin 1 strain is essential for attenuation of enterovirus 71 in the NOD/SCID mouse infection model. J. Virol. **82:**1787–1797. http://dx.doi.org/10.1128/JVI.01798-07.

59. **Chua BH, Phuektes P, Sanders SA, Nicholls PK, McMinn PC.** 2008. The molecular basis of mouse adaptation by human enterovirus 71. J. Gen. Virol. **89:**1622–1632. http://dx.doi.org/10.1099/vir.0.83676-0.

60. **Ong KC, Shimizu H, Nishimura Y, Arita M, Shamala D, Cardosa MJ, Wong KT.** 2008. Phenotypic and genotypic characterization of two mouse adapted enterovirus 71 strains that showed differences in murine CNS infection. Int. J. Infect. Dis. **12:**E74–E74. http://dx.doi.org/10.1016/j.ijid.2008.05.186.

61. **Wang YF, Chou CT, Lei HY, Liu CC, Wang SM, Yan JJ, Su IJ, Wang JR, Yeh TM, Chen SH, Yu CK.** 2004. A mouse-adapted enterovirus 71 strain causes neurological disease in mice after oral infection. J. Virol. **78:**7916–7924. http://dx.doi.org/10.1128/JVI.78.15.7916-7924.2004.

62. **Chernyatina AA, Nicolet S, Aebi U, Herrmann H, Strelkov SV.** 2012. Atomic structure of the vimentin central alpha-helical domain and its implications for intermediate filament assembly. Proc. Natl. Acad. Sci. U. S. A. **109:**13620–13625. http://dx.doi.org/10.1073/pnas.1206836109.

63. **Hermann H, Haner M, Brettel M, Muller S, Goldie KN, Fedtke B, Lustig A, Franke WW, Aebi U.** 1996. Structure and assembly properties of intermediate filament protein vimentin: the role of its head, rod and tail domains. Mol. Biol. Cell **264:**933–953.

64. **Traub P, Scherbarth A, Wiegers W, Shoeman RL.** 1992. Salt-stable interaction of the amino-terminal head region of vimentin with the alpha-helical rod domain of cytoplasmic intermediate filament proteins and its relevance to protofilament structure and filament formation and stability. J. Cell Sci. **101:**363–381.